



MONASH University

**A Printed, Flexible Counter Electrode for Dye Sensitized
Solar Cells**

Jyothi Ramamurthy, B. App. Sci (Hons)

A thesis submitted for the degree of Master of
Philosophy at Monash University in 2018
Science

Copyright notice

© Jyothi Ramamurthy

Abstract

This thesis is centred on developing a flexible counter electrode for use in dye sensitised solar cells (DSSCs) that can be fabricated using scalable printing or coating processes at ambient conditions. In contrast to the materials conventionally used for the DSSC counter electrode, the proposed electrode is made from nickel, a relatively cheap metal, and the conducting polymer poly(3,4-ethylenedioxythiophene) *p*-toluenesulfonate (PEDOT:PTS). Use of this type of scalable deposition process enables comparatively cheap, high volume, rapid production roll to roll techniques to be implemented, serving to drastically reduce both the monetary and energy cost currently associated with fabrication of the DSSC counter electrode. The scalable deposition techniques used in this thesis are bar coating and gravure printing.

Cells made using this alternate counter electrode and utilising the iodide/triiodide redox couple in the electrolyte were characterised using the electrochemical analysis techniques of Electric Impedance Spectroscopy and cyclic voltammetry. Results of this electrochemical analysis indicated that the nickel in the electrode was being degraded, i.e. corroded, by the iodide/triiodide redox couple in the electrolyte. Wet chemistry tests confirmed this theory.

Tests quantifying the amount of swelling that the PEDOT:PTS underwent when submerged in the electrolyte solvent, *methoxy* propionitrile (MPN) were also carried out. The PEDOT:PTS swelled to a maximum mass of 112% of its original mass with MPN over the first nine days and stabilised at approximately 110% of its original mass after 19 days.

It was determined that the tested Ni/PEDOT:PTS counter electrode was incompatible with the iodide/triiodide redox couple. That is to say the experimental Ni/PEDOT:PTS counter electrode cannot be used in a cell utilising the iodide/triiodide redox couple in the electrolyte.

The use of the experimental Ni/PEDOT:PTS counter electrode in a cell employing the cobalt^{II/III} redox couple was briefly explored. It was identified that two components are compatible with one another and there is potential for the Ni/PEDOT test counter electrode to be used in a cell utilising the cobalt^{II/III} redox couple.

Declaration

This thesis contains no material which has been accepted for the award of any other degree or diploma at any university or equivalent institution and that, to the best of my knowledge and belief, this thesis contains no material previously published or written by another person, except where due reference is made in the text of the thesis.

Signature:

Print Name:Jyothi Ramamurthy.....

Date:20/04/2018.....

Acknowledgements

I am sincerely thankful to my supervisors Doug MacFarlane, Bjorn Winther-Jensen, Noel Clark and Fiona Scholes, whose guidance and support from the inception to the completion of this project has enabled me to develop a deep understanding of the subject matter.

Contents

Chapter 1: Introduction and Literature Review.....	9
1.1 Introduction.....	9
1.1.1 Preface.....	9
1.1.2 The Conventional Counter Electrode.....	11
1.1.3 DSSC Efficiency.....	12
1.1.4 The Advantage of Roll to Roll Printed, Flexible DSSC Components.....	12
1.1.5 Overall Goal of Thesis.....	13
1.1.6 Overview of the Thesis.....	14
1.2 Literature Review.....	14
2.1.1 Alternate Counter Electrodes – General.....	14
2.1.2 Alternate Counter Electrodes: Nickel.....	17
2.2 Vapour Phase Polymerisation of Poly(3,4-ethylenedioxythiophene).....	19
Chapter 2: Deposition, Characterisation and Durability of Counter Electrode Materials.....	24
2.1 Nickel Coating Deposition, Characterisation and Durability.....	24
2.1.1 Introduction.....	24
2.1.2 Experimental.....	24
2.1.3 Results and Discussion.....	25
2.2 PEDOT:PTS Deposition and Characterisation.....	33
2.2.1 Experimental.....	33
2.2.2 Results and Discussion.....	34
2.3 Conclusion.....	42
Chapter 3: Electrochemical testing of symmetric and asymmetric cells.....	42
3.1 Introduction.....	42
3.1.1 Electrical Impedance Spectroscopy of Symmetric and Asymmetric cells.....	42
3.1.2 Experimental.....	44
3.1.3 Results and Discussion.....	45
3.1.4 Conclusion.....	52
Chapter 4: Additional testing of the system containing nickel/PEDOT:PTS electrode and iodine based electrolyte.....	54
4.1 Introduction.....	54
4.2 Further electrochemical analysis of the system: Tafel plots.....	54
4.2.1 Experimental.....	55
4.2.2 Results and Discussion.....	56
4.3 Wet chemistry testing to confirm the presence of nickel in iodine based electrolytes.....	59
4.3.1 Experimental.....	59
4.3.2 Results and Discussion.....	60

4.4 Swelling of PEDOT:PTS in methoxypropionitrile.	61
4.4.1 Experimental.....	61
4.4.2 Results and Discussion.....	62
4.5 Conclusion	63
Chapter 5: EIS of a cell containing the nickel/PEDOT:PTS electrode and an electrolyte containing the cobaltII/III redox couple.	65
5.1 Introduction	65
5.1.1 Experimental.....	65
5.1.2 Results and Discussion.....	66
5.1.3 Conclusion.....	68
Chapter 6: Conclusions and Further Work	69
6.1 Conclusions	69
6.2 Future Work.....	71

Chapter 1: Introduction and Literature Review

1.1 Introduction

1.1.1 Preface

Meeting the rising energy demand stemming from both the growth of world population and industrial developments in an environmentally sustainable manner poses a substantial challenge. The projection of world energy demand, by the US Energy Information Administration, is a total growth from the present 14 terawatts towards 25-30 terawatts in 2050 [1]. Renewable energy is vital for a sustainable future and, along with hydropower, wind, and biomass, solar energy is central to this. Most people would be familiar with conventional solar technology, namely crystalline silicon solar cells commonly seen on rooftops of domestic and commercial buildings. These conventional solar cells have become relatively inexpensive in recent times and they perform reliably in the range of approximately 15% to 25% power conversion efficiency.

Dye sensitised solar cells (DSSCs) may be a feasible alternative to conventional silicon solar cells in some applications. DSSCs' potential for low cost and high efficiency means they could play the role of a complimentary technology, to be used in applications to which silicon solar is not suited. The record light to energy conversion reported for a DSSC is 14 % and was achieved in 2015[2]. DSSCs can be fabricated using thin, lightweight and flexible substrates, enabling portability of this energy source. Furthermore, the colour of these solar cells can easily be tuned to deliver the required aesthetics to a specific application.

DSSCs are commonly fabricated by arranging thin film components as shown in Figure 1.1.

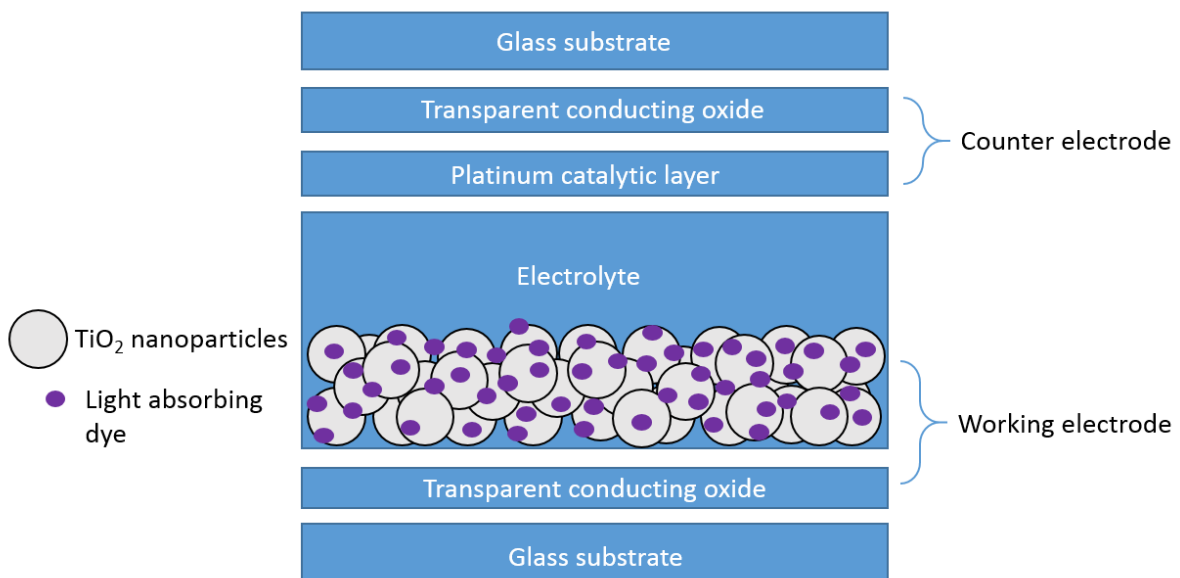


Figure 1.1 Schematic Diagram of a Dye Sensitised Solar Cell

Dye sensitised solar cells typically consist of five components. These are a transparent substrate (usually glass) coated with conductive oxide, a mesoporous titanium oxide layer composed of TiO₂ nanoparticles, a light absorbing dye layer, an electrolyte containing a redox couple and, finally, a counter electrode composed of a transparent conducting oxide and a catalytic material.

Anode, or working electrode

This electrode comprises a transparent substrate, commonly glass, which has been coated with a thin conductive layer[3]. This is usually a transparent conductive oxide, e.g. fluorine tin oxide (FTO) or indium tin oxide (ITO).

Light absorbing layer

A film of n-type semiconductor is layered onto the working electrode, creating a mesoporous structure. This semiconductor is usually titanium dioxide[4] but occasionally another oxide, such as zinc oxide, is used [5-7]. A monolayer of light absorbing dye is adsorbed onto this mesoporous structure, sensitising the film for light harvesting. The colour of the DSSC can be tuned by varying this light absorbing dye[8].

Cathode, or counter electrode

Similar to the working electrode, the counter electrode is commonly made from glass coated with a conducting material, i.e. ITO or FTO, and sputtered with platinum[4]. Platinum acts as a catalyst to reduce the active species in the redox electrolyte. The role of the counter electrode is to transfer electrons arriving from the external circuit back to the redox electrolyte.

Electrolyte

The electrolyte contains a redox couple which regenerates the dye contained in the cell during cell operation. It also fills the space between the working electrode and the counter electrode, providing electrical contact between the anode and the cathode. The electrolyte acts as the potential barrier necessary for photovoltaic conversion. Earlier studies into DSSCs utilised electrolytes based on the iodide/triiodide redox couple[9]. However, more recently, electrolytes containing alternate redox couples have been used with good results[10-13].

Each component of a DSSC is dependent on the other materials contained in the same cell. If one component is changed, e.g. the dye, either electrode or the composition of the electrolyte, the entire system will require optimisation to maximise cell performance.

Upon exposure to sunlight, dye molecules within a DSSC absorb light energy, causing electrons to be injected into the conduction band of the mesoporous oxide layer. These electrons are adsorbed on to the oxide layer.

Electron donation from the redox couple in the electrolyte subsequently restores the dye to its original state, circumventing the recapture of any electrons liberated from the dye. The liberated electron passes through the outer circuit to the counter electrode. The electrolyte within the cell is then regenerated through a platinum catalysed reduction reaction at the counter-electrode. The circuit is completed by electron migration through the external load. The DSSC cell generates electrical power from light without undergoing any overall permanent chemical transformation.

1.1.2 The Conventional Counter Electrode

The counter electrode is a critical element of DSSCs. As previously mentioned, the role of the counter electrode in a DSSC is to transfer electrons arriving from the external circuit of the cell back to the redox electrolyte, in addition to carrying the photocurrent over the width of each solar cell. The counter electrode of a DSSC most commonly consists of a catalytic coating of platinum on a transparent conducting oxide (TCO) coated glass substrate deposited using either sputtering or thermal decomposition of hexachloroplatinic acid. Fluorine-doped tin oxide is most commonly used as the TCO, however indium-doped tin oxide (ITO) coated glass is occasionally implemented [14]. The counter electrode, which must be substantially conductive and exhibit a low overvoltage for reduction of the redox couple contained in the electrolyte, has crucial influence on the photovoltaic performance, long-term stability and fabrication cost of DSSCs[15].

Papageorgiou *et al.* conducted an in depth study into platinum as an iodide/triiodide electrocatalyst for aqueous and organic media[16]. In particular, the kinetics of reduction of triiodide and the mass transfer limitation on the photocurrent of a cell was studied. This study investigated both deposition methods of platinum, i.e. thermal deposition from hexachloroplatinic acid and sputtering. It was found that the thermally deposited platinum was more stable and showed a higher exchange current for the triiodide/iodide redox couple.

Subsequently, Hauch and Georg[17] used impedance spectra to investigate R_{ct} (resistance to charge transfer) of platinized TCO counter electrodes prepared by either electron beam evaporation, sputtering or thermal deposition from hexachloroplatinic acid. The R_{ct} was measured with various electrolyte solvents in a symmetric two-electrode cell. A 450 nm thick sputtered platinum electrode gave the lowest R_{ct} of 0.05 ohm cm^2 , with an acetonitrile solvent to improve the diffusion coefficient of the triiodide ion. The thickness of the platinum layer correlated to the capacitance on the electrode, i.e. a thicker platinum layer showed higher capacitance, with scanning electron microscopy (SEM) revealing a porous structure.

Although the glass/TCO/platinum counter electrode has served the field well until now, there are some serious limitations associated with use of this electrode in its current form. Platinum is one of the most expensive rare metals and adds significant cost to the total production price of the cell. Also, conventional platinum electrodes are fabricated using either sputtering of platinum or deposition from platinum acid [16]. These techniques require either temperatures of around 450°C for 15 minutes[18] or vacuum conditions. Both of these methods

consume a large amount of energy. Furthermore, the use of very high temperatures excludes the possibility of use of flexible, plastic substrates required for reel-to-reel printing, i.e. plastic substrates cannot withstand such high temperatures. This will be further discussed later in this chapter.

There have been reports in the literature of platinum being unstable in a DSSC electrolyte solution containing the iodide/triiodide redox couple[19, 20]. In 2012 Syrokostas *et al.* [20] reported a drop of up to 40% in the current density for triiodide reduction after storage of platinum electrodes prepared by electrodeposition and thermal decomposition of hexachloroplatinic acid solutions after storage in an I^-/I_3^- electrolyte solution for 24 hours. Olsen *et al.*[19] reported linear sweep voltammetry experiments showing that the electrocatalytic activity of vapour deposited Pt on FTO coated glass plates is drastically reduced after immersion for 24 hours in an I^-/I_3^- electrolyte solution.

Conversely, Hinsch *et al.* published a study showing the conventional DSSC system performance in accelerated aging tests; the cells showed electrochemical stability equivalent to at least 10 years outdoor operation[21]. However, UV stabilization of the conventional electrolyte with MgI_2 was employed to achieve this long term stability. Jung *et al.* also reported that the conventional system is stable[22].

1.1.3 DSSC Efficiency

The first practical DSSC was reported in 1991 by O'Regan and Gratzel [3]. Attempts to use dye sensitised photoelectrochemical cells in energy conversion had been made previously, but the efficiencies of these devices were deemed to be too low to be practicable[23, 24]. O'Regan and Gratzel's reported cell had a light-to-energy conversion yield of 7.1-7.9% in simulated solar light and 12% in diffuse daylight. The authors attributed the success of their cell to the high surface area of the titanium dioxide layer of the working electrode, achieved by use of semiconductor films of nanometer-sized particles. The increased surface area of the mesoporous structure allowed vastly more dye molecules to be adsorbed directly onto the electrode surface when compared to the smooth surfaces that had been used previously. Hence, more light was absorbed by the cell and cell efficiency increased.

The current efficiency record for DSSCs was achieved in 2015 and stands at 14%[2].

DSSCs have potential as an important and impactful renewable energy technology. However, common deposition methods used in laboratories, such as spin coating and electrodeposition, are not scalable and therefore are not translatable to industrial production.

1.1.4 The Advantage of Roll to Roll Printed, Flexible DSSC Components

Developing alternate DSSC components that enable roll to roll fabrication on a flexible substrate is an attractive prospect as implementation of such fabrication would both simplify and lower the cost of cell production. There have been a number of studies conducted into the fabrication of flexible DSSCs[25-27]. In 2006, Ito *et al.*[27]

fabricated a flexible DSSC by replacing the commonly used glass electrode substrates with titanium foil as the working electrode substrate and polyethylene naphthalate (PEN) as the counter electrode substrate. In this case, the counter electrode consisted of purchased pre-prepared indium tin oxide (ITO) coated PEN with a platinum catalytic coating. Later, in 2008, Kuang *et al.*[26] described a fully flexible DSSC utilising TiO₂ nanotubes as the working electrode and, similarly to Ito *et al.*, a platinum coated ITO-PEN counter electrode. The platinum here was deposited using sputtering, which requires vacuum conditions. This thesis specifically examines flexible, roll to roll printed or coated fabrication at ambient conditions.

At ambient conditions, roll to roll printed fabrication is a low monetary and energy cost fabrication method. Using this method of fabrication commercially would aid in making DSSC solar technology inexpensive and, therefore, increase consumer uptake. Fabrication at ambient conditions, reducing production energy cost, is favourable from an sustainability perspective. A flexible substrate is essential when using roll to roll printed fabrication methods as the substrate, or web, must be able to bend and flex around the rollers of the printer.

Physical attributes introduced by fabricating DSSCs using thin film roll to roll printing, i.e. sleek form factor, light weight and flexibility, would open up this technology for use in many applications that it is not necessarily suited to currently. These physical attributes would make printed DSSCs ideal for use in portable consumer products, i.e. integration into tents or backpacks.

1.1.5 Overall Goal of Thesis

The overall goal of this thesis was to investigate the physical and electrochemical properties of a printed, flexible novel DSSC counter electrode fabricated using nickel and poly(3,4-ethylene dioxythiophene) *p*-toluene sulfonate deposited via wholly scalable methods. Figure 1.2 shows the structure of PEDOT:PTS.

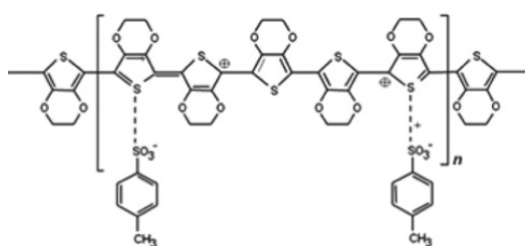


Figure 1.2 Diagram of PEDOT:PTS structure[28].

Two generations of this nickel/PEDOT-PTS counter electrode are considered in this thesis. The first generation consists of a nickel coating coated on flexible polyethylene tetrathalate (PET) film and then printed with PEDOT:PTS. The second generation consists of PEDOT:PTS being printed directly onto flexible metallic nickel film. The PEDOT:PTS fills the role of the conventionally used platinum, while nickel is used in place of the FTO conductive coating, or a glass/FTO substrate, for generation one and two respectively.

Application of this counter electrode would aid in reducing both energy and monetary cost of DSSC production. Furthermore, since the proposed counter electrode could be produced using scalable printing processes, high throughput rapid production would be enabled.

1.1.6 Overview of the Thesis

This chapter, Chapter One, contains a general introduction to DSSC components, along with a review of the literature. The literature available on DSSCs is vast and only a small selection could be presented here. As such, the literature discussed in this thesis is a selection of what was deemed to be the most relevant to this study.

Chapter Two contains a description, characterisation and discussion of the deposition, using scalable printing and coating techniques that can be easily adopted industrially, of a conducting material (nickel) and a catalytic material (PEDOT:PTS) onto insulating and flexible PET film.

Chapter Three is a description and analysis of electrochemical testing, namely electrical impedance spectroscopy, obtained from cells containing an experimental counter electrode consisting of flexible nickel foil and printed PEDOT:PTS, with a typical DSSC electrolyte utilising the iodide/triiodide redox couple.

Chapter Four is an account and discussion of further testing that was conducted on the experimental counter electrode discussed in Chapter Three. This further testing includes wet chemistry tests, a swelling test of the conducting polymer in organic solvent using a technique employing a quartz crystal microbalance and further electrochemical testing, specifically cyclic voltammetry to construct Tafel plots.

Chapter Five is a brief explanation and interpretation of the nickel foil and PEDOT:PTS counter electrode used in conduction with an alternative DSSC electrolyte containing the $\text{Co}^{2+/3+}$ redox couple.

Chapter Six contains the conclusion of this thesis and describes further work that could be undertaken in this field.

1.2 Literature Review

2.1.1 Alternate Counter Electrodes – General

Since the late 1990s, research has been conducted into the development of an alternate DSSC counter electrode[29, 30]. Most investigations into alternate counter electrode options involve replacement of either the traditional substrate[31] or catalytic coating[32-35], with some studies researching different options for both components[36, 37].

A 2000 study conducted by Lindstrom *et al.*[37] detailed the development of a counter electrode consisting of an ITO-coated PET film substrate, coated with a mixture of graphite powder and carbon black using doctor blading. The ITO coating overcomes the sheet resistance (R_s) issue of the insulating plastic substrate. The maximum energy conversion efficiency observed in a cell made using this counter electrode was 4.9% at 100 mW cm^{-2} light intensity.

Fang *et al.* published a study in 2005 detailing the construction of counter electrodes based on flexible metal and plastic substrates, specifically stainless steel sheet, nickel sheet, polyester film and polyethylene naphthalate film coated with ITO (ITO-PEN)[31]. Platinum particles were sputtered onto all four substrates and, for comparison, an FTO coated glass sheet. DSSCs were fabricated using these counter electrodes to investigate their performance. The cells made using counter electrodes based on stainless steel and nickel had energy conversion efficiencies comparable to that of the counter electrode based on the commonly used FTO glass sheet and it was suggested that they may feasibly be used as flexible replacements for the conductive glass sheet.

Multiple research groups have investigated the replacement of sputtered platinum with conducting polymers as the catalytic coating on FTO coated glass[38-42]. Conducting polymers are suited to this application as they tend to have a microporous morphology, which is advantageous to the catalytic activity required. In fact, it has been published that conjugated polymers, such as PEDOT derivatives, actually out-perform platinum in DSSCs due to their higher catalytic properties for reduction of the triiodide ion at the counter electrode[43] when iodide/triiodide based electrolytes are used. The reason for this is that these conjugated polymer films tend to have a higher porosity than platinum films. As such, a greater surface area is available for catalytic activity.

Doping of conducting polymers by counter-ions such as SO_4^{2-} , ClO_4^- and Cl^- may further increase their porosity[32], further increasing the surface area available to catalytic activity. A 2002 study found that the use of counter electrodes fabricated using PEDOT doped with the tosylate anion gave cells with efficiencies of 4.6%, more than double that of cells incorporating counter electrodes fabricated using poly(3,4-ethylenedioxythiophene) polystyrene sulfonate (PEDOT:PSS) in the same study[44]. Chen *et al.* investigated many different dopants of PEDOT:PSS in 2007, including dimethyl acetamide (DMAc), dimethyl formamide (DMF), dimethyl carbonate (DMC) and dimethyl sulfoxide (DMSO)[45], with the aim of increasing conductivity of the films. This group also added a small amount of carbon black to their PEDOT films to enhance roughness, again increasing the surface area available for catalytic activity. The combination of counter electrode materials giving the highest efficiency was DMSO-PEDOT:PSS (0.1wt% carbon black) (power conversion efficiency of 5.8 %).

A 2009 study by Sirimanne *et al.* explored the use of vapour phase polymerised PEDOT:PTS as both a redox catalyst and electron conductor in DSSCs[43]. In this case, PEDOT:PTS was coated on either glass, titanium foil or PEN. The authors note that the resistance of PEDOT:PTS films increased with decreasing film thickness, i.e. the resistance of a 20 μm continuous film was 4 Ω/square , while the resistance of a 0.5 μm continuous film was 60 Ω/square .

More recently, Chen *et al.*[36] developed a pure carbon counter electrode for use in DSSCs. The substrate of the cell was a flexible graphite sheet onto which activated carbon was applied to the substrate using doctor blading. This counter electrode combined the high conductivity of the flexible graphite with the high catalytic property of activated carbon to achieve low series and charge transfer resistance. Cells containing these pure carbon counter electrodes achieved maximum conversion efficiencies of 6.46% and 5%, respectively. Pt/FTO glass based devices, fabricated for comparison during this study, achieved conversion efficiencies of 6.37% and 2.91% for the same cell areas.

In 2010, Pringle *et al.* showed that the stability of DSSCs fabricated using an ITO-PEN/PEDOT counter electrode and an ionic liquid electrolyte was promising. In this case, PEDOT was deposited using electrodeposition, with relatively short deposition times that may be suitable to reel-to-reel printing. These cells showed very little decrease in efficiency over a period of four and a half months storage in air with no additional sealing[39].

In 2011, Wang *et al.* conducted an extensive study into alternate DSSC counter electrodes. The group fabricated DSSC counter electrodes using three nanomaterials as catalysts to replace expensive platinum[46]. These nanomaterials were titanium carbide (TiC), tungsten oxide (WO₂) and vanadium nitride (VN). These nanomaterials were deposited on three different substrates; bare glass, titanium foil and polyimide. The insulating bare glass was coated with a conductive carbon layer to enable conductivity. Conductive carbon was chosen to replace the FTO conductive layer because of its excellent electrical conductivity, low sheet resistance and good adhesion to glass. The three conducting substrates and experimental catalytic materials were tested in all nine possible combinations. Cells containing counter electrodes using a glass/FTO substrate and all three experimental catalytic materials were also tested. Power conversion efficiencies for the cells containing counter electrodes using polyimide film substrate were comparatively lower than the other cells because the high surface resistance of polyimide resulted in low current and fill factors. For the cells containing glass/conductive carbon substrate the power conversion efficiencies decreased to 80%-90% that of cells using the conventional glass/FTO substrate due to a decrease in fill factor. The combination of experimental counter electrode conducting substrate and experimental catalytic material that yielded the best power conversion efficiency was Ti/TiC, with an efficiency of 7.15%. The other two Ti substrate combinations had the second and third highest power conversion efficiencies of the group, due to the high conductivity and resulting low sheet resistance of the Ti foil substrate.

The Gratzel group has used electrodeposition of conducting polymers from ionic liquids to control the morphology of the resulting films[38, 40]. These films were used as DSSC counter electrodes in cells yielding power conversion efficiencies of 8-9 %, comparable to cells incorporating standard FTO/platinum counter electrodes. The authors claim that electropolymerised PEDOT films are highly porous with a uniform grain size dictating catalytic activity. The highly porous microstructure affords a high specific surface area. The ionic

liquids work as a supporting electrolyte in the polymer synthesis and alter reaction pathways, dictating the resulting microstructure.

Recently Lee *et al.* [47] reported on a flexible, paper based DSSC counter electrode using a graphene dot and PEDOT:PSS composite as a catalytic conducting material. The investigators postulate that the graphene dot/PEDOT:PSS composite fills the micro-pores in the commercially available A4 printing paper substrate, leading to improved carrier transport in the electrode and enhanced efficiency. Sheet resistance of films was found to be reduced by almost an order of magnitude in films containing 30% graphene dots in PEDOT:PSS when compared to pristine PEDOT:PSS films. In turn, efficiencies of cells incorporating these graphene dot/PEDOT:PSS films were higher. However, the efficiencies of cells made using PEDOT:PSS, 30% graphene dot/PEDOT:PSS and platinum sputtered onto paper in the counter electrodes were 5.14%, 7.36% and 8.46% respectively, indicating that platinum is the most effective catalytic material of the three. After bending of the paper electrodes 150 times, the performance of cells containing the graphene dot/PEDOT:PSS were well preserved while the performance of the cell made using the sputtered platinum decreased by 45% after the same test.

2.1.2 Alternate Counter Electrodes: Nickel

Nickel has been identified as a possible replacement for the TCO in DSSC counter electrodes due to its high conductivity and low cost. Nickel, in various forms described here, has been investigated for this application. Unless stated, these experimental electrodes were tested in cells containing electrolytes base on the iodide/triiodide redox couple.

Ma *et al.* in 2004 conducted a study on several variations of the typical DSSC counter electrode [48]. While all the counter electrodes examined during this study employed sputtered platinum as their catalytic material, substrates tested included sheets of stainless steel, nickel, aluminium, and copper, along with the ITO coated polymers polystyrene, polyethylene, polyester and polyethylene naphthalate. Various physical parameters of the substrate materials were characterised. Sheet resistance of all the counter electrode substrates were measured; the metal film substrates had much lower sheet resistances than the ITO coated polymer substrates, i.e. R_s was approximately three orders of magnitude lower. The corrosion stabilities of the metal and plastic substrates in an iodide/triiodide electrolyte solution were also examined after three months of exposure at both room temperature and 60 °C. It was observed that copper and aluminium foils corroded in the electrolyte and polystyrene film dissolved slightly in the electrolyte. All the other substrates tested were deemed to be stable. When DSSCs were fabricated employing the test substrates as counter electrode materials, it was found that the ITO-PEN substrate yielded the highest power conversion efficiency of 5.39%, with the stainless steel and nickel substrates second and third highest respectively (5.24% and 5.13%). The control cell using FTO coated glass as the counter electrode substrate had a power conversion efficiency of 5.94%. The main influencing factor in whether or not a material was a good counter electrode substrate in this study was the magnitude of sheet

resistance of the material. Materials with high sheet resistance yielded lower power conversion efficiencies when they were employed as counter electrode substrates in dye sensitised solar cells.

A study was conducted by Jiang *et al.* and published in 2010[49]. This study involved the use of surface-nitrided nickel foil and nickel particle films as counter electrodes in DSSCs. The nickel was surface-nitrided at 450°C for two hours in a flowing ammonia atmosphere. DSSCs fabricated using counter electrodes made from nickel foil had energy conversion efficiencies of 0.09%, while the use of nitrided nickel foil gave an efficiency of 5.68% and nitrided nickel particle film gave an efficiency of 8.31%. The authors postulate that DSSCs fabricated using a nitrided nickel particle film counter electrode were the most efficient due to the film's porous morphology, allowing for a higher active surface area.

A number of research groups have used nickel materials, i.e. nickel oxide, nickel selenide, etc. as the catalytic material in a DSSC counter electrode. A separate conducting substrate, usually FTO coated glass, was used in these studies.

In early 2011, Sun *et al.* reported on their study into nickel sulfide electrodeposited onto FTO coated glass for use as DSSC counter electrodes[50]. A periodic potential reversal (PR) technique was employed to assist the electrodeposition. This PR technique involved imposing periodic anodic bias to dissolve the excess nickel metal and ensure the preparation of single-component nickel sulphide. The authors reported that NiS deposited this way displayed remarkable electrochemical stability. This was deduced by testing these electrodes in DSSCs containing an electrolyte based on the iodide/triiodide redox couple over a 10 day period. Over the testing period, the cells experienced a slight decrease in charge transfer resistance; this was extrapolated to indicate stability. DSSCs made using these counter electrodes achieved power conversion efficiencies of 6.8%. For comparison, devices made using conventional Pt coated counter electrodes achieved power conversion efficiencies of 7.0%.

Similarly, in 2013, Ku *et al.* fabricated transparent nickel sulphide counter electrodes[51]. In this case, these electrodes were developed specifically for use with an electrolyte based on the thiolate/disulphide redox couple. The nickel sulphide in this study was also deposited using the PR technique. While the electrode showed a high transparency, up to 90% in the spectral absorption range of the dye used (N719 dye), extremely poor fill factors were achieved. As such, the authors were disappointed in the photovoltaic performance of conversion efficiency 4.1%.

Wang *et al.* investigated nickel oxide as an efficient counter electrode catalyst for dye sensitised solar cells in 2013[52]. In this study, nickel oxide was used in conjunction with PEDOT:PSS in a dye sensitised solar cell with a maximum power conversion efficiency of 7.58%. Specifically, nickel oxide powder was mixed with PEDOT:PSS solution to form a homogenous paste, which was deposited onto FTO coated glass using doctor blading. DSSCs

fabricated using this counter electrode, along with DSSC incorporating counter electrodes of NiO, PEDOT:PSS and platinum on FTO/glass were fabricated and characterised. The DSSC containing a counter electrode incorporating platinum had the highest power conversion efficiency of 8.7%, followed by the DSSC containing a counter electrode incorporating NiO/PEDOT:PSS at a 48:1 ratio. The cells containing counter electrodes incorporating PEDOT:PSS and NiO had power conversion efficiencies of 4.6 and 0.28 respectively.

In 2014 a further study was published on the use of nickel sulphide as a counter electrode component for DSSCs; this time the nickel sulphide was supported by nickel foil. A facile one-step hydrothermal process was used to prepare a NiS/Ni₃S₂ nanorod composite that grows directly on nickel foil. Power conversion efficiencies achieved by DSSCs employing the experimental nickel based counter electrode and the conventional FTO/Pt electrode were 6.2% and 7.6% respectively.

A study published in 2015 by Jia *et al.*[53] detailed the integration of a transparent nickel selenide counter electrode into a DSSC. Nickel selenide was deposited onto FTO/glass through a facile solvo-thermal reaction, i.e. a nickel selenide solution was spin coated onto clean FTO glass, which was then dried at 80°C for 30 minutes. The power conversion efficiency of this cell, 8.88%, actually exceeded the power conversion efficiency of the control cell, i.e. a cell incorporating a FTO coated glass/platinum electrode. The power conversion efficiency of the control cell was 8.13%. To further characterise the catalytic activity of the nickel selenide electrode, field emission scanning electron microscopy was conducted on the nickel selenide coating. It was found that the nickel selenide exists in aggregations of particles, with particle size around 200 nm. The aggregation exhibits a porous structure, which explains the improved reaction speed of this counter electrode when compared to the non-porous FTO/glass/Pt electrode.

2.2 Vapour Phase Polymerisation of Poly(3,4-ethylenedioxythiophene)

Poly(3,4-ethylenedioxythiophene) (PEDOT) is a robust intrinsically electrically conducting polymer. PEDOT has been widely used in the printed electronics industry, in particular for anti-static coatings, organic light emitting diodes (OLEDs) and organic photovoltaics (OPVs). PEDOT can be prepared either electrochemically or by oxidative chemical polymerisation. The oxidative chemical polymerisation technique has an advantage over electrochemical preparation in that it does not require support from a conducting substrate[54]. The conductivity of these conducting polymers can be ascribed to the delocalisation of *pi* electrons over the polymeric backbone. The resulting positive charges on the polymer chains are stabilised by dopant anions that bind to the polymer, balancing the net charge.

Oxidative chemical polymerisation can be carried out either through wet chemistry methods or through vapour phase polymerisation (VPP). VPP as a synthetic route to PEDOT was first reported in 2003[33] and involves, first, a substrate being coated or patterned with an acidic oxidant. The coated substrate is then exposed to monomer vapour, i.e. 3,4-ethylenedioxythiophene (EDOT) monomer in the case of PEDOT synthesis. Polymerisation of the

EDOT monomer takes place on the surface of the substrate in the pattern in which the oxidant has been applied to the substrate, forming a PEDOT film doped with the anion of the oxidant.

A 2004 study by Winther-Jensen *et al.*[55] detailed a mechanism for a cleavage side reaction for the polymerisation of EDOT monomer under acidic conditions that reduced the conductivity of the resulting PEDOT film. It was suggested that occurrence of these side reactions could be circumvented by simply raising the pH of the reaction conditions using an additive such as pyridine.

Subsequently in 2011, Winther-Jensen *et al.* studied the use of a diurethane diol to control domain formation and inhibit cleavage reactions during VPP of PEDOT:PTS[54]. During this study, the investigators prepared PEDOT:PTS films in the presence of the mediators pyridine, diurethane diol, 2-oxazolidinone, 3-methyl-2-oxazolidinone, *N*-ethylurethane, 2-hydroxyethyl-*N*-methylcarbamate and imidazole. Oxidant/inhibitor solutions were spin coated onto glass and VPP polymerisation was carried out using EDOT monomer. The films were then characterised using optical microscopy, surface resistivity measurements and UV-visible spectrophotometry. While cyclic voltammograms of the PEDOT:PTS films deposited using different polyurethanes showed very similar features, it was found that the conductivity results from the film deposited using diurethane diol stood out when compared to the other films, including the film deposited using pyridine. The conductivity of this film peaked at >1000 S/cm at an addition molar ratio of 1.8%. Furthermore, optical microscopy of the films indicated that the films deposited using diurethane diol were more homogenous than the other films. A reason for this phenomenon was not suggested in the paper.

It is important to find alternative materials to those traditionally used in the manufacture of counter electrodes, i.e. FTO coated glass and platinum, in order to make the commercial production of DSSCs feasible. The literature indicates that two qualities, among others, are crucial in a DSSC counter electrode. The conducting substrate of a counter electrode material should exhibit low sheet resistance and the catalytic layer of the material should be highly porous to enable a high surface upon which catalytic activity can take place. The use of a flexible substrate will allow the option of reel-to-reel printing of the cells, and the replacement of platinum in the cell by a more cost-effective material will make DSSCs much more affordable. In the proposed alternate cathode, the use of expensive materials is circumvented. Platinum, which is one of the most expensive rare metals available, is replaced with the inexpensive conducting polymer, PEDOT-PTS as the catalytic layer in the cathode. The standard FTO coated glass, which accounts for approximately 60% of the total cell cost[56], is replaced with the less expensive nickel. The deposition techniques used in this study are translatable to large scale, roll to roll printing.

Chapter 1 References

1. Mozaffari, S., M.R. Nateghi, and M.B. Zarandi, *An overview of the Challenges in the commercialization of dye sensitized solar cells*. Renewable & Sustainable Energy Reviews, 2017. **71**: p. 675-686.

2. Kakiage, K., *et al.*, *Highly-efficient dye-sensitized solar cells with collaborative sensitization by silyl-anchor and carboxy-anchor dyes*. *Chemical Communications*, 2015. **51**(88): p. 15894-15897.
3. Oregan, B. and M. Gratzel, *A LOW-COST, HIGH-EFFICIENCY SOLAR-CELL BASED ON DYE-SENSITIZED COLLOIDAL TiO₂ FILMS*. *Nature*, 1991. **353**(6346): p. 737-740.
4. Gratzel, M., *Dye-sensitized solar cells*. *Journal of Photochemistry and Photobiology C-Photochemistry Reviews*, 2003. **4**(2): p. 145-153.
5. Zhang, W., *et al.*, *Facile construction of nanofibrous ZnO photoelectrode for dye-sensitized solar cell applications*. *Applied Physics Letters*, 2009. **95**(4): p. 3.
6. Keis, K., *et al.* *Nanostructured ZnO electrodes for dye-sensitized solar cell applications*. in *1st International Conference on Semiconductor Photochemistry (SP-1)*. 2001. Glasgow, Scotland: Elsevier Science Sa.
7. Kakiuchi, K., E. Hosono, and S. Fujihara, *Enhanced photoelectrochemical performance of ZnO electrodes sensitized with N-719*. *Journal of Photochemistry and Photobiology a-Chemistry*, 2006. **179**(1-2): p. 81-86.
8. Zhang, K., *et al.*, *High-Performance, Transparent, Dye-Sensitized Solar Cells for See-Through Photovoltaic Windows*. *Advanced Energy Materials*, 2014. **4**(11): p. 7.
9. Boschloo, G. and A. Hagfeldt, *Characteristics of the Iodide/Triiodide Redox Mediator in Dye-Sensitized Solar Cells*. *Accounts of Chemical Research*, 2009. **42**(11): p. 1819-1826.
10. Mathew, S., *et al.*, *Dye-sensitized solar cells with 13% efficiency achieved through the molecular engineering of porphyrin sensitizers*. *Nature Chemistry*, 2014. **6**(3): p. 242-247.
11. Daeneke, T., *et al.*, *High-efficiency dye-sensitized solar cells with ferrocene-based electrolytes*. *Nature Chemistry*, 2011. **3**(3): p. 211-215.
12. Lu, J.F., *et al.*, *Alternate redox electrolytes in dye-sensitized solar cells*. *Chinese Science Bulletin*, 2012. **57**(32): p. 4131-4142.
13. Yanagida, S., Y.H. Yu, and K. Manseki, *Iodine/Iodide-Free Dye-Sensitized Solar Cells*. *Accounts of Chemical Research*, 2009. **42**(11): p. 1827-1838.
14. Hoshikawa, T., *et al.*, *Impedance analysis of internal resistance affecting the photoelectrochemical performance of dye-sensitized solar cells*. *Journal of the Electrochemical Society*, 2005. **152**(2): p. E68-E73.
15. Wu, J.H., *et al.*, *Counter electrodes in dye-sensitized solar cells*. *Chemical Society Reviews*, 2017. **46**(19): p. 5975-6023.
16. Papageorgiou, N., W.F. Maier, and M. Gratzel, *An iodine/triiodide reduction electrocatalyst for aqueous and organic media*. *Journal of the Electrochemical Society*, 1997. **144**(3): p. 876-884.
17. Hauch, A. and A. Georg, *Diffusion in the electrolyte and charge-transfer reaction at the platinum electrode in dye-sensitized solar cells*. *Electrochimica Acta*, 2001. **46**(22): p. 3457-3466.
18. Pringle, J.M., *et al.*, *PEDOT-Coated Counter Electrodes for Dye-Sensitized Solar Cells*. *Australian Journal of Chemistry*, 2009. **62**(4): p. 348-352.
19. Olsen, E., G. Hagen, and S.E. Lindquist, *Dissolution of platinum in methoxy propionitrile containing LiI/I⁻*. *Solar Energy Materials and Solar Cells*, 2000. **63**(3): p. 267-273.
20. Syrokostas, G., *et al.*, *Degradation mechanisms of Pt counter electrodes for dye sensitized solar cells*. *Solar Energy Materials and Solar Cells*, 2012. **103**: p. 119-127.
21. Hinsch, A., *et al.*, *Long-term stability of dye-sensitised solar cells*. *Progress in Photovoltaics*, 2001. **9**(6): p. 425-438.
22. Jung, H.S. and J.K. Lee, *Dye Sensitized Solar Cells for Economically Viable Photovoltaic Systems*. *Journal of Physical Chemistry Letters*, 2013. **4**(10): p. 1682-1693.
23. Alonso, N., *et al.*, *DYE SENSITIZATION OF CERAMIC SEMICONDUCTING ELECTRODES FOR PHOTOELECTROCHEMICAL CONVERSION*. *Revue De Physique Appliquee*, 1981. **16**(1): p. 5-10.
24. Matsumura, M., Y. Nomura, and H. Tsubomura, *DYE-SENSITIZATION ON PHOTOCURRENT AT ZINC-OXIDE ELECTRODE IN AQUEOUS-ELECTROLYTE SOLUTION*. *Bulletin of the Chemical Society of Japan*, 1977. **50**(10): p. 2533-2537.

25. Kang, M.G., *et al.*, *A 4.2% efficient flexible dye-sensitized TiO₂ solar cells using stainless steel substrate*. *Solar Energy Materials and Solar Cells*, 2006. **90**(5): p. 574-581.
26. Kuang, D., *et al.*, *Application of highly ordered TiO₂ nanotube arrays in flexible dye-sensitized solar cells*. *ACS Nano*, 2008. **2**(6): p. 1113-1116.
27. Ito, S., *et al.*, *High-efficiency (7.2%) flexible dye-sensitized solar cells with Ti-metal substrate for nanocrystalline-TiO₂ photoanode*. *Chemical Communications*, 2006(38): p. 4004-4006.
28. Kim, J.Y., *et al.*, *Highly Conductive and Transparent Poly(3,4-ethylenedioxythiophene):p-Toluene Sulfonate Films as a Flexible Organic Electrode*. *Japanese Journal of Applied Physics*, 2009. **48**(9): p. 6.
29. Murakoshi, K., *et al.*, *Solid state dye-sensitized TiO₂ solar cell with polypyrrole as hole transport layer*. *Chemistry Letters*, 1997(5): p. 471-472.
30. He, J.J., *et al.*, *Dye-sensitized nanostructured p-type nickel oxide film as a photocathode for a solar cell*. *Journal of Physical Chemistry B*, 1999. **103**(42): p. 8940-8943.
31. Fang, X.M., *et al.*, *Flexible counter electrodes based on metal sheet and polymer film for dye-sensitized solar cells*. *Thin Solid Films*, 2005. **472**(1-2): p. 242-245.
32. Li, Z.P., *et al.*, *Facile electropolymerized-PANI as counter electrode for low cost dye-sensitized solar cell*. *Electrochemistry Communications*, 2009. **11**(9): p. 1768-1771.
33. Balraju, P., *et al.*, *Dye sensitized solar cells (DSSCs) based on modified iron phthalocyanine nanostructured TiO₂ electrode and PEDOT:PSS counter electrode*. *Synthetic Metals*, 2009. **159**(13): p. 1325-1331.
34. Lee, K.M., *et al.*, *Highly porous PProDOT-Et-2 film as counter electrode for plastic dye-sensitized solar cells*. *Physical Chemistry Chemical Physics*, 2009. **11**(18): p. 3375-3379.
35. Suzuki, K., *et al.*, *Application of carbon nanotubes to counter electrodes of dye-sensitized solar cells*. *Chemistry Letters*, 2003. **32**(1): p. 28-29.
36. Chen, J.K., *et al.*, *A flexible carbon counter electrode for dye-sensitized solar cells*. *Carbon*, 2009. **47**(11): p. 2704-2708.
37. Lindstrom, H., *et al.*, *A new method for manufacturing nanostructured electrodes on plastic substrates*. *Nano Letters*, 2001. **1**(2): p. 97-100.
38. Ahmad, S., *et al.*, *Efficient Platinum-Free Counter Electrodes for Dye-Sensitized Solar Cell Applications*. *Chemphyschem*. **11**(13): p. 2814-2819.
39. Pringle, J.M., V. Armel, and D.R. MacFarlane, *Electrodeposited PEDOT-on-plastic cathodes for dye-sensitized solar cells*. *Chemical Communications*. **46**(29): p. 5367-5369.
40. Ahmad, S., *et al.*, *Dye-sensitized solar cells based on poly (3,4-ethylenedioxythiophene) counter electrode derived from ionic liquids*. *Journal of Materials Chemistry*. **20**(9): p. 1654-1658.
41. Kitamura, K. and S. Shiratori, *Layer-by-layer self-assembled mesoporous PEDOT-PSS and carbon black hybrid films for platinum free dye-sensitized-solar-cell counter electrodes*. *Nanotechnology*. **22**(19): p. 6.
42. Li, Q.H., *et al.*, *Application of microporous polyaniline counter electrode for dye-sensitized solar cells*. *Electrochemistry Communications*, 2008. **10**(9): p. 1299-1302.
43. Sirimanne, P.M., *et al.*, *Towards an all-polymer cathode for dye sensitized photovoltaic cells*. *Thin Solid Films*. **518**(10): p. 2871-2875.
44. Saito, Y., *et al.*, *Application of poly(3,4-ethylenedioxythiophene) to counter electrode in dye-sensitized solar cells*. *Chemistry Letters*, 2002(10): p. 1060-1061.
45. Chen, J.G., H.Y. Wei, and K.C. Ho, *Using modified poly(3,4-ethylene dioxythiophene): Poly(styrene sulfonate) film as a counter electrode in dye-sensitized solar cells*. *Solar Energy Materials and Solar Cells*, 2007. **91**(15-16): p. 1472-1477.
46. Wang, Y.D., *et al.*, *Several highly efficient catalysts for Pt-free and FTO-free counter electrodes of dye-sensitized solar cells*. *Journal of Materials Chemistry*, 2012. **22**(9): p. 4009-4014.
47. Lee, C.P., *et al.*, *A paper-based electrode using a graphene dot/PEDOT:PSS composite for flexible solar cells*. *Nano Energy*, 2017. **36**: p. 260-267.
48. Ma, T.L., *et al.*, *Properties of several types of novel counter electrodes for dye-sensitized solar cells*. *Journal of Electroanalytical Chemistry*, 2004. **574**(1): p. 77-83.

49. Jiang, Q.W., et al., *Surface-Nitrided Nickel with Bifunctional Structure As Low-Cost Counter Electrode for Dye-Sensitized Solar Cells*. Journal of Physical Chemistry C. **114**(31): p. 13397-13401.
50. Sun, H.C., et al., *Dye-sensitized solar cells with NiS counter electrodes electrodeposited by a potential reversal technique*. Energy & Environmental Science, 2011. **4**(8): p. 2630-2637.
51. Ku, Z.L., et al., *Transparent NiS counter electrodes for thiolate/disulfide mediated dye-sensitized solar cells*. Journal of Materials Chemistry A, 2013. **1**(2): p. 237-240.
52. Wang, H., W. Wei, and Y.H. Hu, *NiO as an Efficient Counter Electrode Catalyst for Dye-Sensitized Solar Cells*. Topics in Catalysis, 2014. **57**(6-9): p. 607-611.
53. Jia, J.B., et al., *Transparent nickel selenide used as counter electrode in high efficient dye-sensitized solar cells*. Journal of Alloys and Compounds, 2015. **640**: p. 29-33.
54. Winther-Jensen, B., et al., *Inhomogeneity Effects in Vapor Phase Polymerized PEDOT: A Tool to Influence Conductivity*. Macromolecular Materials and Engineering, 2011. **296**(2): p. 185-189.
55. Winther-Jensen, B. and K. West, *Vapor-phase polymerization of 3,4-ethylenedioxythiophene: A route to highly conducting polymer surface layers*. Macromolecules, 2004. **37**(12): p. 4538-4543.
56. Wang, Y.D., et al., *Several highly efficient catalysts for Pt-free and FTO-free counter electrodes of dye-sensitized solar cells*. Journal of Materials Chemistry. **22**(9): p. 4009-4014.

Chapter 2: Deposition, Characterisation and Durability of Counter Electrode Materials

2.1 Nickel Coating Deposition, Characterisation and Durability

2.1.1 Introduction

The proposed DSSC cathode investigated here consisted of nickel used in conjunction with the conducting polymer PEDOT:PTS. This chapter is primarily concerned with the first generation of this cathode, which utilises flexible polyethylene terephthalate (PET) film as substrate. This flexible substrate was first coated with nickel and then printed with PEDOT:PTS.

Nickel was deposited in the form of a commercially available formulation, MG Chemicals Super Shield Conductive Coating (USA). This product was formulated by the supplier for intended use as a radio frequency shielding material and consisted of nickel flakes in an organic binder.

The roughness and thickness of the nickel coating was characterized using profilometry, and the coating was sanded to reduce its roughness. The nickel coating was also characterized using scanning electron microscopy (SEM) coupled with energy dispersive X-ray spectroscopy.

Finally, the durability of the nickel coating in two solutions was tested by immersing glass coated with nickel into two separate electrolyte solutions. One of these electrolyte solutions used an isopropanol based solvent system and the other solution used an ionic liquid based solvent system.

2.1.2 Experimental

The MG Chemicals Super Shield Conductive Coating nickel formulation was coated onto the PET substrate (DuPont, 125 micron) using an RK Print Meter Bar Coater (UK). Bar number 0, colour coded white, was used for this coating. This bar had a wire diameter of 0.002 inch/0.05 mm. The coated PET was then left in a working fume hood at ambient conditions for 24 hours to allow the coating to cure.

The bar coated nickel coating was imaged and analysed using a scanning electron microscope (SEM) (Philips XL30 Field Emission Scanning Electron Microscope) coupled with energy dispersive X-ray spectroscopy (EDS). The surface resistivity of the coating was measured using a four point probe (Jandel 3000, UK).

The thickness and roughness of the coated nickel formulation was determined using a Dektak 6M stylus profilometer. Since profilometry is very problematic to carry out on flexible materials, the commercial nickel formulation was coated onto glass, using a method identical to that used to coat the nickel formulation onto PET. The coating was cured at ambient conditions inside a working fume hood for 24 hours and characterised.

To reduce the roughness of the nickel coating, the coating was polished using wet/dry silicon carbide

sandpaper of 600, 1200 and 2500 grit successively. After polishing with sandpaper, the surface of the nickel coating was wiped very gently with an ethanol soaked paper towel to remove any residual nickel dust.

Experiments were conducted to test the durability of the commercial nickel coating in two different typical DSSC electrolyte solutions. Samples of glass substrate and samples of PET substrate were coated with the nickel formulation. These samples were then immersed in an ionic liquid based electrolyte solution[1] or in an isopropanol based electrolyte solution[2]. Both electrolytes contained the iodide/triiodide (I^-/I_3^-) redox couple as the redox mediator. The ionic liquid electrolyte comprised guanidine thiocyanate, iodine and 4-*tert*-butylpyridine (0.5 M), with the bulk of the volume made from a 13:7 mixture of 1-methyl-3-propylimidazolium iodide and 1-ethyl-3-methylimidazolium thiocyanate. The organic solvent electrolyte comprised iodine, 1-methyl-3-propyl imidazolium iodide and *N*-methylimidazole in an isopropanol solvent. The reduced species in the redox couple, I^- , regenerates the photo-oxidised dye, while the oxidised species, I_3^- , is reduced by the counter electrode.

The samples were visually observed at regular intervals to gauge the durability of the electrode, with both glass and PET substrate, over time in the organic solvent based electrolyte and the ionic liquid based electrolyte.

2.1.3 Results and Discussion

The type of bar coating used to coat the commercial nickel formulation on to PET, and on to glass for profilometry, was a simple method involving application of accurate, reproducible layers of material onto substrates. A pattern of identically shaped grooves in the bar were made by precision drawn stainless steel wire wound onto a stainless steel rod. The bar was drawn down the length of a printing bed, applying the coating to the substrate. The resulting wet film thickness was precisely controlled by the spaces between the grooves of the wound wire on the bar and the depth of the grooves. In this type of coating, the wet film thickness can be varied by using bars wound with varying wire thicknesses and winding patterns.

Figure 2.1 depicts the type of bar coater used.



Figure 2.1 RK Print Meter Bar Coater (<http://www.rkprint.co.uk>)

Figure 2.2 and 2.3 show images of the bar coated nickel formulation obtained by SEM. The bright areas of the image were found to be nickel (analysed as nickel using EDS) and the dark areas were found to be acrylic binder (analysed as oxygen and carbon using EDS). The grey areas are likely to be nickel with a thin layer of binder on the surface.

Figure 2.2 shows that a large proportion of the coating's surface consisted of the insulating organic binder. The surface resistivity of the coating was between two and five ohms per square. The low surface resistivity of the coating indicated that, although the binder made up a large area of the coating's surface, the nickel flakes interconnected laterally throughout the coating to afford good conductivity. As shown in Figure 2.3, nickel flake diameters ranged from approximately one micron to five microns in diameter.

Figures 2.2 and 2.3 depict scanning electron microscopy (SEM) images of the surface of the bar coated nickel material on PET.

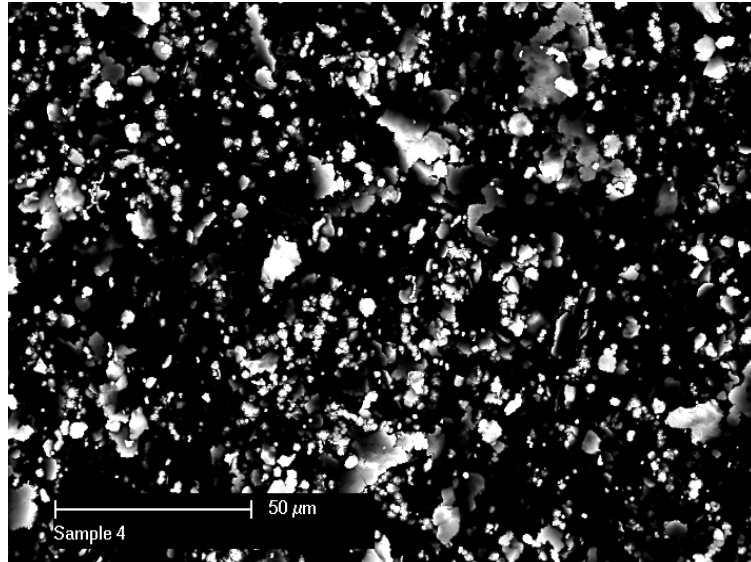


Figure 2.2 SEM image of bar coated nickel formulation on PET

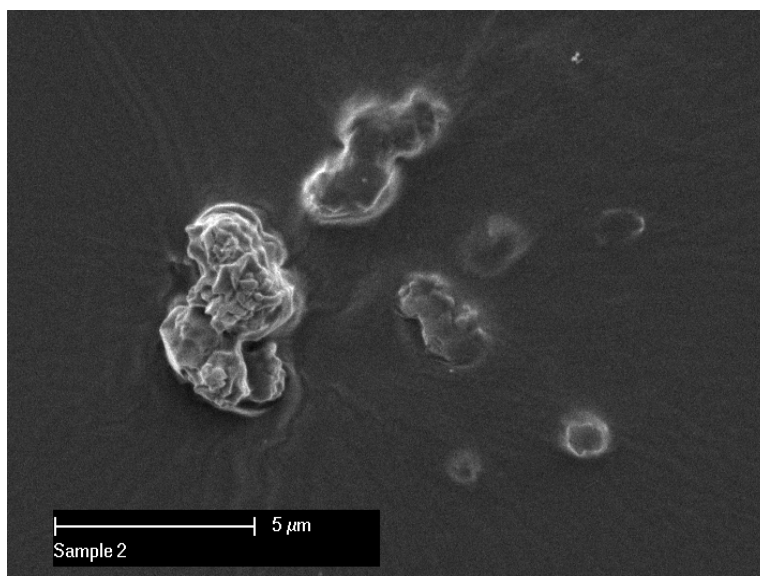


Figure 2.3: SEM image of nickel flakes in bar coated nickel formulation showing nickel flake size.

Profilometry characterization was carried out using samples with the nickel formulation coated onto glass. It was assumed that the thickness data obtained for the nickel formulation coated onto glass could be extrapolated to the same formulation, coated in the same manner, on flexible PET substrate.

The mean thickness of the nickel coating on glass was found to be 24 microns. The maximum roughness of the nickel coating was found to be two microns, i.e. two microns between the highest peaks and lowest troughs. A maximum roughness of two microns was deemed too rough for use as a counter electrode in a DSSC as the risk of these peaks in the nickel coating making contact with the working electrode and creating a short circuit was high.

Polishing of the coating was carried out by hand and, although every effort was made to ensure the polishing process was uniform, the process was subject to a small amount of variation between each sample and, indeed, areas of the same sample. If the polishing was carried out using an electric sander, on a research scale, the sander would need to be operated by a human so the same type of error would be encountered. If this process was implemented industrially, an automated sander/polisher could be implemented and this uniformity issue could be circumvented to a degree. However, since there is substantial inherent size variation between individual nickel particles within the formulation, it is not possible to totally eliminate variation between samples or areas of the same sample.

It was essential to be very gentle when cleaning samples after sanding. If vigorous rubbing of the sample with an ethanol soaked towel occurred to remove dust generated during sanding, the coating was removed.

After polishing, the maximum roughness of the coating was reduced to one micron. Traces of the profilometer scans of the unpolished nickel coating surface and the polished nickel coating surface, showing the roughness of each coating, are shown in Figures 2.4 and 2.5 respectively.

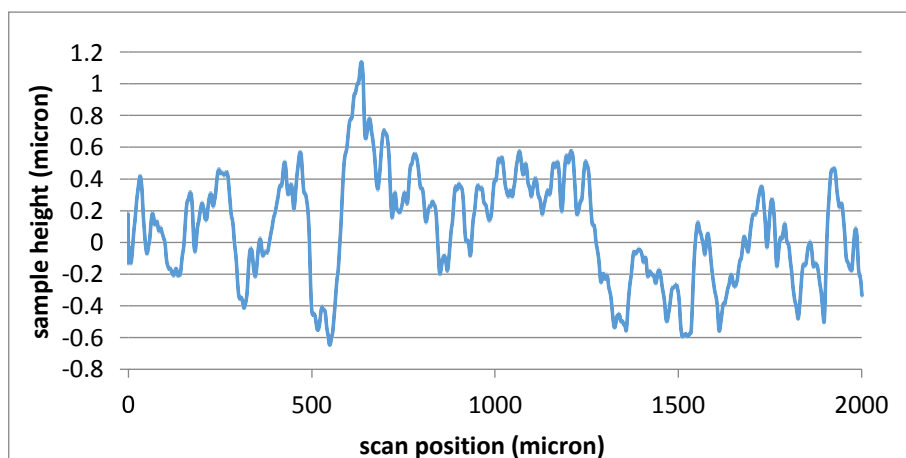


Figure 2.4: Profilometry trace of the unpolished nickel coating

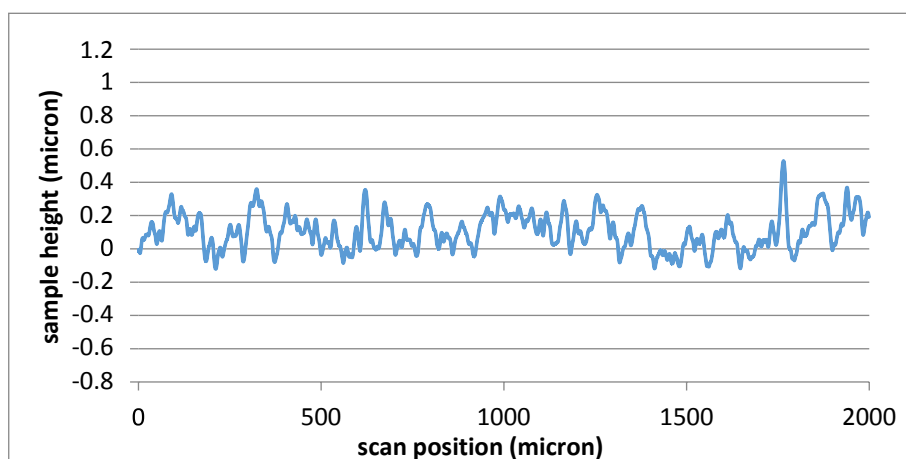


Figure 2.5: Profilometry trace of the polished nickel coating

Samples of glass coated with the nickel formulation and samples of PET coated with the nickel formulation were immersed in an ionic liquid based electrolyte solution[1] or in an isopropanol based electrolyte solution[2]. Both electrolytes contained the iodide/triiodide (I^-/I_3^-) redox couple as the redox mediator. The ionic liquid electrolyte comprised guanidine thiocyanate, iodine and 4-*tert*-butylpyridine (0.5 M), with the bulk of the volume made from a 13:7 mixture of 1-methyl-3-propyl

imidazolium iodide and 1-ethyl-3-methylimidazolium thiocyanate. The organic solvent electrolyte comprised iodine, 1-methyl-3-propyl imidazolium iodide and *N*-methylimidazole in an isopropanol solvent. The reduced species in the redox couple, I^- , regenerates the photo-oxidised dye, while the oxidised species, I_3^- , is reduced by the counter electrode.

The samples were visually observed at regular intervals to gauge the durability the electrode, with both glass and PET substrate, over time in the organic solvent based electrolyte and the ionic liquid based electrolyte.

The coating on all the samples that had been immersed in the isopropanol based electrolyte solution dissolved within 16 days. Figures 2.6 and 2.7 illustrate the degradation in isopropanol based electrolyte of these glass and PET substrates respectively.



Figure 2.6 Degradation of nickel coating on glass substrate after 16 days immersion in an isopropanol based electrolyte solution. The two samples are duplicates of each other.



Figure 2.7 Degradation of nickel coating on PET substrate after 16 days immersion in an isopropanol based electrolyte solution. The two samples are duplicates of each other.

In contrast to these results, after 109 days of immersion in the ionic liquid electrolyte, the nickel/acrylic binder coating on both glass and PET was still intact and showed no signs of degradation. Figures 2.8 and 2.9 illustrate the condition of these coatings after 109 days in ionic liquid based electrolyte on glass substrate and PET substrate respectively.



Figure 2.8 Nickel coating on glass substrate intact after 109 days immersion in an ionic liquid based electrolyte solution. The two samples are duplicates of each other.

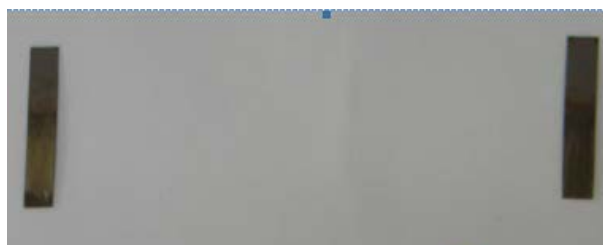


Figure 2.9 Nickel coating on PET substrate intact after 109 days immersion in an ionic liquid based electrolyte solution. The two samples are duplicates of each other.

Although the sample on the left in Figure 2.9 appears to show some degradation, the colour difference along the sample is actually dark brown electrolyte solution resting on the sample surface.

It was garnered from these test results that the nickel coating was durable in this ionic liquid electrolyte solution.

2.2 PEDOT:PTS Deposition and Characterisation

2.2.1 Experimental

PEDOT:PTS was deposited on the nickel, i.e. either nickel sheet or nickel coated onto PET, using gravure printing of an oxidant, followed by a vapour phase polymerisation process. The nickel sheet used was purchased from Aldrich (Australia) and was 0.125 mm thick and 99.9% pure. Details of the oxidant are listed in the following paragraphs. Single sheet gravure printing was used and was carried out using an RK Print Gravure Proofer(UK) at a speed of 5.

The PEDOT:PTS was formed using a method known as vapour phase polymerisation[4]. During this vapour phase polymerisation (VPP) process an oxidant solution, along with the urethane, diurethane diol, was deposited on either coated nickel or nickel sheet using gravure printing, as detailed above. Diurethane diol was selected as an additive to the oxidant solution as it has been shown to increase the homogeneity and conductivity of PEDOT:PTS films[5].

This oxidant consisted of a commercial iron(III) tosylate solution (Clevios, Germany) in butanol with the inhibitors polyethylene glycol (PEG 20000, Sigma Aldrich, Australia) and diurethanediol (DUDO, Sigma Aldrich, Australia). DUDO, sold as polyurethane diol is a dimer with a molecular weight of 320

g/mol and was purchased as an 88% solution in water. It is described by Sigma-Aldrich as an aliphatic urethane of proprietary composition and the structure is not given for commercial reasons. The addition ratio of PEG and DUDO to iron tosylate solution was 0.033 g (predissolved in 0.2 mL of deionised water and 0.031 g respectively). The sample was then rinsed very carefully and gently using ethanol.

A QCM200 Quartz Crystal Microbalance was used to quantify the mass of PEDOT:PTS gravure printed onto the nickel coated PET substrates. First, PEDOT:PTS was coated onto a 5 MHz AT-cut quartz crystal. Oxidant, as described in 2.2.1 was spin coated (WS-400B-8NPP/Lite, Laurel, USA) at 2000 rpm onto the quartz crystal. PEDOT:PTS was then formed using VPP. Here, oxidant was spin coated rather than printed as it was impossible to gravure print using a quartz crystal as the substrate due to the small size and rigidity of the crystal. Cyclic voltammograms of the coated quartz crystal at a scan rate of 5 mV/s were produced using a conventional three electrode system made up of the coated quartz crystal acting as a working electrode, a gold counter electrode and a KCl reference electrode. A 0.1 M sodium tosylate solution was used as the electrolyte in this system.

Printing experiments were conducted on PET/coated nickel samples on which either one, two or three layers of oxidant were printed to vary the PEDOT:PTS thickness on the samples. Polymerisation of all these samples took place after all oxidant layers were printed.

All samples for analysis of PEDOT:PTS mass were taken from the first centimetre of the printed area which, due to the inherent variation in thickness profile of the single sheet gravure print, was the thickest area of printed PEDOT:PTS.

Flexible nickel foil of 0.125 mm thickness and 99.9 % purity was purchased from Aldrich (Australia). Similar printing experiments to those conducted on PET/coated nickel samples were conducted. However, in this case, only one layer of PEDOT:PTS was printed on each sample.

2.2.2 Results and Discussion

Gravure printing is an intaglio printing process, meaning that the image to be printed is engraved onto an image carrier. It is most commonly employed as a roll to roll printing technique but can also be performed using single sheet printing. Gravure printing is commonly used for long, high quality print runs such as magazines, mail-order catalogues, packaging and postage stamps. In its simplest form, gravure printing consists of a two part system: a coating roller and a support roller. The coating roller is engraved with a pattern made from small wells that hold ink and is partially immersed in a bath of ink. Any excess ink resting on the surface of the roller, not contained in the wells, is removed from the roller using a doctor blade immediately before the roller is brought into contact with the substrate. The support roller, which guides the substrate, and the coating roller are forced into contact. The support

roller commonly has a hard rubber coating and gives way, i.e. compresses, for the coating roller. The gravure pattern engraved onto the coating roller is transferred to the substrate upon contact in the form of discrete dots of ink. To form a continuous film, the applied ink must sufficiently wet the substrate so that all the discrete ink dots join together. For most applications in which gravure printing is used, a continuous film of ink is not required and the discrete dots imparted by this type of printing serve to provide a sharp printed image. A schematic diagram of the gravure printing process is shown in Figure 2.10.

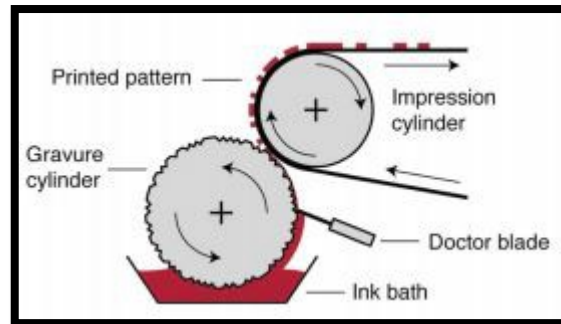


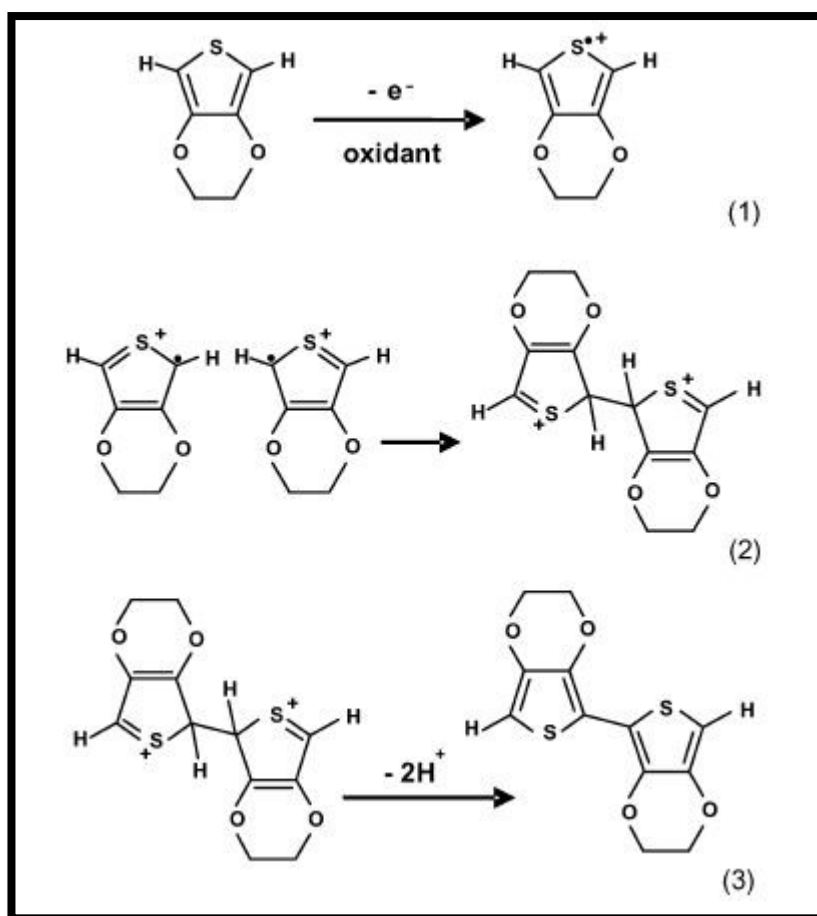
Figure 2.10 Schematic diagram of the roll to roll gravure printing press[3]



Figure 2.11 RK Print Gravure Proofer (<http://www.rkprint.co.uk>)

Figure 2.11 shows a gravure proofer identical to the instrument used in these experiments. The engraved pattern of this gravure proofer was located on a stainless steel bed over which the support roller, made of a compressible rubber material, was drawn. The substrate was attached to the support roller and forced into contact with the engraved bed as the roller moved towards the opposite end of the bed. Ink, i.e. oxidant solution, was manually deposited in a thin strip in front of the support roller before each single sheet print was carried out. The ink was then spread by the support roller to fill the engraved wells on the print bed and, when the substrate contacted the engraved stainless steel bed, ink in the pattern required was transferred to the substrate.

The oxidant was a brownish-yellow bulk solution that appeared almost colourless after printing on the nickel coating. Immediately after printing, the entire sample was placed inside a sealed vessel (VPP chamber) containing approximately 0.2 mL of EDOT monomer. The VPP chamber and its contents were placed in an oven and heated to 60°C for 40 minutes. During this time the EDOT monomer vaporised, with the vapour filling the entire volume of the VPP chamber. At this stage of the process, the vaporised monomer came into contact with the oxidant that had been printed during the previous step, undergoing oxidant induced polymerisation. A mechanism for this polymerisation process has been proposed in the literature and is included in Figure 2.12.



[6]

Figure 2.12 Proposed mechanism for EDOT oxidant induced polymerisation reaction. (1) EDOT is oxidised to form an EDOT cation; (2) EDOT cations stabilise by forming dimers; (3) Proton scavenging causes dimers to be deprotonated. Cycle repeats multiple times to form a conjugated PEDOT chain.

When polymerisation was complete, the printed area on the nickel was composed of PEDOT:PTS, together with any remaining unreacted oxidant. The printed area was blueish-green in colour as a result of the combination of the dark blue PEDOT:PTS film and yellow unreacted oxidant. After rinsing, only the dark blue PEDOT:PTS coating remained on the sample in the pattern in which the oxidant had been originally printed on the substrate at the commencement of the VPP process.

Since the purpose of this experimental procedure is simply to quantify the mass of PEDOT:PTS deposited onto nickel during this study, using spin coating as the deposition method rather than gravure printing should not have a bearing on results. Cyclic voltammetry was used to quantify the mass of PEDOT:PTS gravure printed onto the nickel coated PET substrates. The resulting cyclic voltammogram is shown in Figure 2.13.

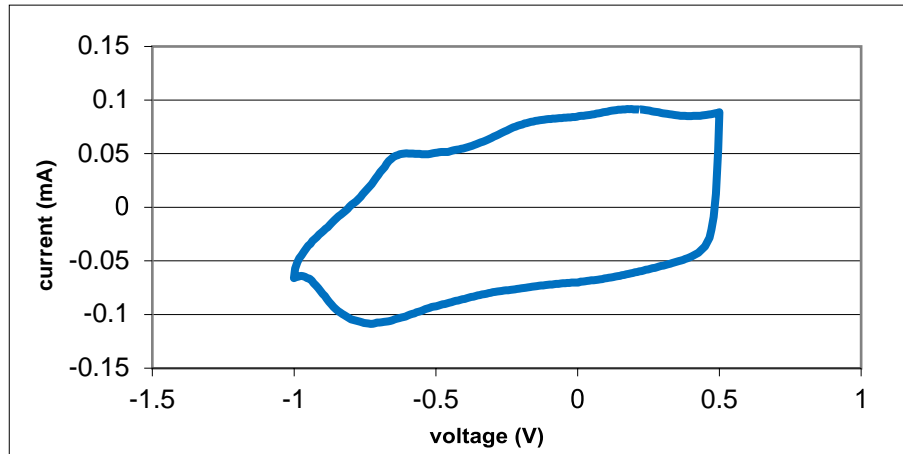


Figure 2.13 Quartz crystal cyclic voltammetry scan, scan rate 5 mV/s, 0.1 M sodium tosylate electrolyte, KCl reference electrode

The Sauerbrey equation was used to determine the mass of PEDOT on the quartz crystal using the cyclic voltammogram data.

Sauerbrey showed in 1959 that the thickness of a film deposited onto the electrodes of a piezoelectric quartz resonator is inversely proportional to the resonance frequency[7]. The Sauerbrey equation is defined as:

$$\Delta f = -\frac{2f_0^2}{A\sqrt{\rho_q\mu_q}}\Delta m.$$

Where:

f_0 = resonance frequency (Hz)

Δf = frequency change (Hz)

Δm = mass change (g)

A = piezoelectrically active crystal area (area between electrodes, cm²)

ρ_q = density of quartz ($\rho_q = 2.648 \text{ g/cm}^3$)

μ_q = shear modulus of quartz for AT-cut crystal ($\mu_q = 2.947 \times 10^{11} \text{ g/cm s}^{-2}$)

The Sauerbrey equation treats the film as an extension of the quartz crystal thickness. As such, whether the equation is applicable or not is dependent on certain conditions being met; the deposited film must be rigid and evenly distributed across the crystal and the frequency change $\Delta f/f$ must be less than 0.02.

From the above equation, the mass of PEDOT:PTS printed per farad was found to be 1590 micrograms.

The change in current at E_{we}/V , where E_{we} is the stationary potential for the impedance measurement and V is the potential amplitude of the sine signal, vs SCE = 0.1 V was noted and this change in current was divided by the scan rate to give the total capacitance for the total electrode area. This value was then scaled down to give the capacitance per cm^2 of electrode material. This capacitance was subsequently related to experimental samples to determine the amount of PEDOT:PTS printed the samples.

The nature of gravure printing is such that, when single sheet printing (as opposed to continuous, roll to roll printing) is used, the ink is printed in a wedge shape, i.e. with the ink layer being thicker at the beginning of the printed sheet than at the end of the printed sheet. Printed thickness is important when depositing a conducting polymer to act as a catalytic material in a DSSC. It is known that, unlike platinum which is most commonly non-porous with catalytic activity occurring primarily on the surface of the material, catalytic activity in conducting polymers usually occurs within the entire thickness of material due to their highly porous structure.

Figure 2.14 shows the mass of PEDOT:PTS printed on the nickel coated PET substrate when one layer of oxidant was printed. Samples 1 – 12 were printed using identical experimental conditions, detailed in Section 2.2.1.

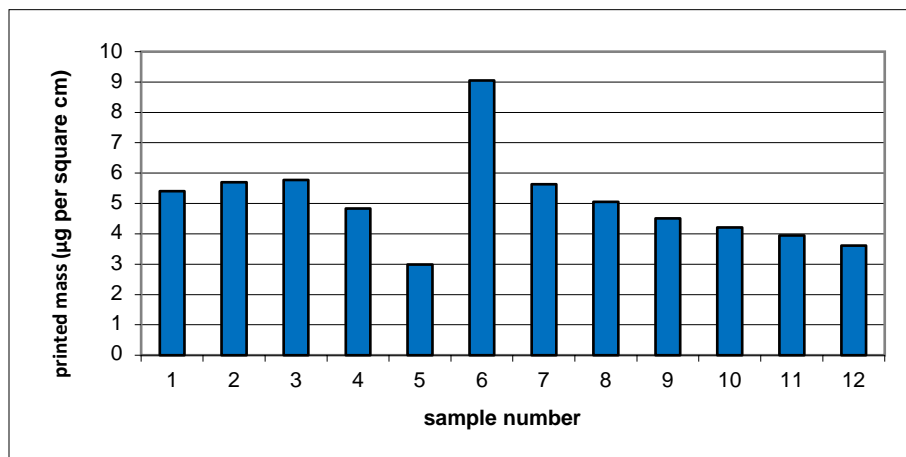


Figure 2.14 Mass of PEDOT:PTS on samples determined using the QCM method. PEDOT:PTS on PET/nickel substrate, scan rate 5 mV/s, 0.1 M sodium tosylate electrolyte, KCl reference electrode

The amount of PEDOT:PTS deposited on the PET/nickel substrate was not reproducible between samples. When one layer of oxidant was printed, the amount of PEDOT:PTS deposited onto the substrate ranged from 3.0 to 9.0 micrograms per cm². When two layers of oxidant were printed, the amount of PEDOT:PTS deposited ranged from 5.4 to 7.4 micrograms. When three layers of oxidant were printed, between 6.6 and 14.7 micrograms were printed. Although there was a general trend relating the number of layers of oxidant deposited to the PEDOT:PTS film thickness, the process lacked the reproducibility required to be useful to a meaningful investigation.

The largest contributor to the lack of reproducibility of the results shown in Figure 2.14 is likely to be the intrinsic roughness of the printed nickel coating. The roughness of the nickel coating influences the mass of oxidant solution printed on a sample and several factors play a role in this parameter. The nature of gravure printing is such that ink transfer from the engraved wells to the substrate will only occur when the substrate makes physical contact with the print bed. Any troughs of the nickel coating would not have made contact with the print bed and, thus, no ink was transferred to these areas. In

addition, the polishing of the samples, which was done by hand, would have varied slightly between each sample. Furthermore, variations in the size of the nickel particles on each sample would cause differences in the sample roughness, irrespective of the consistency of the sample polishing.

Even in the unlikely case that the amount of oxidant printed on separate samples was identical, an amount of unreacted oxidant remained on samples after the vapour phase polymerisation process was completed, as evidenced by the greenish blue colour of the printed area before rinsing with ethanol. Conversion of the total oxidant printed on each sample to PEDOT:PTS was not complete and it is possible that the reaction may not have proceeded to the same point each time it was carried out. In cases of samples being printed with more than one layer of oxidant, the EDOT monomer may have not penetrated the thick oxidant layer, resulting in even more remaining unreacted oxidant. If polymerisation of EDOT took place on the surface of the sample, the sample would then have been coated with a polymer layer, making penetration of EDOT monomer to the oxidant below problematic.

All of the factors above combined resulted in irreproducible results with respect to the final mass of PEDOT:PTS present on each sample. In further studies, the VPP process could be carried out after each oxidant layer was printed, with subsequent layers of oxidant being printed on the surface of the PEDOT:PTS layer. However, the lack of reproducibility seen in the samples with only one layer of PEDOT:PTS indicate that this method change alone would not solve the reproducibility problem.

In an attempt to overcome the reproducibility problem encountered when depositing PEDOT:PTS using the aforementioned gravure printing/VPP polymerisation method, PEDOT:PTS was deposited on flexible, smooth nickel sheet instead of the rough nickel formulation coated onto PET film. The same process as that used previously was used to deposit PEDOT:PTS. However, significant surface variations within samples were eliminated by eliminating the inherent roughness of the nickel layer.

PEDOT:PTS was gravure printed on this nickel foil to determine if using foil, rather than printed nickel formulation on PET, would give more reproducible results. The film thickness was characterised using the method described in Section 2.2.1. The parameters of scan rate, electrolyte and the reference electrode remained the same as the previous experiments. The results are shown in Figure 2.15.

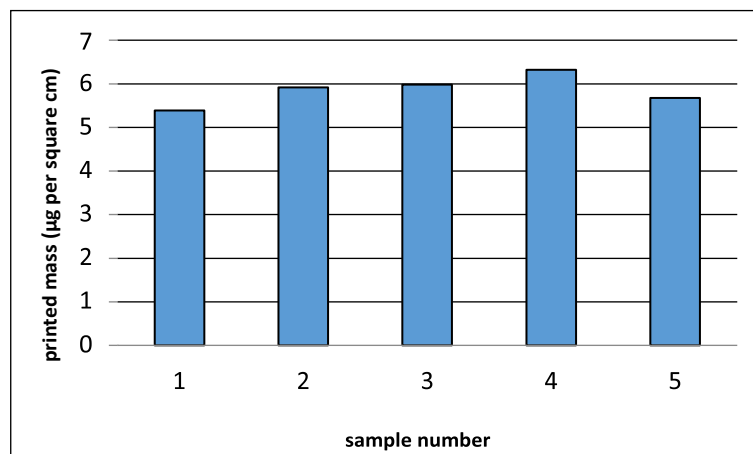


Figure 2.15 Mass of PEDOT:PTS on samples determine using QCM method. PEDOT:PTS on nickel sheet, scan rate 5 mV/s, 0.1 M sodium tosylate electrolyte, KCl reference electrode

The results from this experiment were much more reproducible than the results from previous experiments conducted on samples fabricated using the commercial nickel/binder formulation. When one layer of oxidant was printed, the amount of PEDOT:PTS deposited onto the substrate ranged from 5.4 to 6.3 micrograms per cm².

It was decided that, in the subsequent electrochemical testing of this system, the system would be simplified to increase the likelihood of meaningful results being obtained. Further electrochemical testing was conducted using the simplified electrode, i.e. fabricated from this purchased nickel foil printed with PEDOT:PTS rather than the PET/nickel coated/PEDOT:PTS printed electrode described above. This served to eliminate inconsistencies arising from the nickel surface roughness, inherent nickel particle size variation particle size variation and inconsistencies when polishing.

2.3 Conclusion

Through this investigation into the deposition, characterisation and durability of the nickel metal and PEDOT:PTS conducting polymer proposed as cathode materials, some parameters required for their application were determined. SEM imaging showed that the MG Chemicals nickel coating contained relatively planar nickel particles in diameters ranging from approximately 1 micron to 5 micron. It was found that, when the commercial MG Chemicals nickel formulation was bar coated onto flexible PET to act as conducting DSSC counter electrode substrate, an electrolyte with a typical organic solvent such as isopropanol degraded the nickel coating by dissolving the organic binder in the coating. The nickel coating was found to be durable in an electrolyte employing an ionic liquid solvent (a 13:7 blend of 1- methyl-3-propyl imidazolium iodide and 1-ethyl-3-methylimidazoliumthiocyanate).

PEDOT:PTS was deposited using a VPP process. Deposition via gravure printing of one, two and three layers of VPP oxidant were examined, with polymerisation taking place after all oxidant layers had been printed. However, when depositing multiple layers of oxidant, it may be more effective to carry out the polymerisation step between deposition of each individual layer of oxidant. This method change would increase the likelihood of the majority of oxidant on the sample being reacted. A QCM method was used to quantify the amount of PEDOT:PTS deposited on nickel surfaces using gravure printing.

The nickel surfaces investigated in this chapter were both the commercially available nickel coating and the smoother flexible nickel sheet. PEDOT:PTS deposited onto the flexible nickel sheet was found to be far more reproducible than that deposited onto the commercial nickel coating. This is due to the roughness of the commercial nickel coating. It can be concluded that, regardless of care taken when polishing the bar coated nickel coating, there will always be some variability present in the coating profile. Film roughness is inherent because of this inherent variability in nickel flake size within the coating formulation. Going forward in this study, flexible nickel sheet was used as the counter electrode conducting substrate to eliminate this variability.

Chapter 2 References

1. Wang, P., et al., *A binary ionic liquid electrolyte to achieve $\geq 7\%$ power conversion efficiencies in dye-sensitized solar cells*. Chemistry of Materials, 2004. **16**(14): p. 2694-2696.
2. Wang, P., et al., *Gelation of ionic liquid-based electrolytes with silica nanoparticles for quasi-solid-state dye-sensitized solar cells*. Journal of the American Chemical Society, 2003. **125**(5): p. 1166-1167.
3. www.tappi.org
4. Winther-Jensen, B., et al., *Vapor phase polymerization of pyrrole and thiophene using iron(III) sulfonates as oxidizing agents*. Macromolecules, 2004. **37**(16): p. 5930-5935.
5. Winther-Jensen, B., et al., *Inhomogeneity Effects in Vapor Phase Polymerized PEDOT: A Tool to Influence Conductivity*. Macromolecular Materials and Engineering, 2011. **296**(2): p. 185-189.
6. Fabretto, M., et al., *The role of water in the synthesis and performance of vapour phase polymerised PEDOT electrochromic devices*. Journal of Materials Chemistry, 2009. **19**(42): p. 7871-7878.
7. Sauerbrey, G., *VERWENDUNG VON SCHWINGQUARZEN ZUR WAGUNG DUNNER SCHICHTEN UND ZUR MIKROWAGUNG*. Zeitschrift Fur Physik, 1959. **155**(2): p. 206-222.

Chapter 3: Electrochemical testing of symmetric and asymmetric cells

3.1 Introduction

After examining the experimental results obtained in Chapter Two, it was decided that some changes would be made to the system that was used previously. Instead of using the commercial formulation of nickel flakes in an acrylic binder coated onto a PET film employed in the initial tests detailed in Chapter 2, a flexible nickel foil was used as the conducting substrate of the DSSC counter electrode. This change was implemented to circumvent variations and inconsistencies arising from the roughness of the polished bar coated nickel coating. Instead, a nickel foil of 0.125 mm thickness was used (Aldrich, Australia).

The electrolyte used for electrochemical testing was also changed at this point in the project. The electrolyte that had been used up until this point was taken from the literature[1] and contained iodine (0.2 M), 4-*tert*-butylpyridine (0.5 M) and guanidine thiocyanate (0.14 M) in a 13:7 mixture of 1-methyl-3-propylimidazolium iodide and 1-ethyl-3-methylimidazolium thiocyanate. This ionic liquid based electrolyte was used in Chapter Two of this study due to incompatibility of the previously used commercial nickel coating with an organic solvent based electrolyte. The nickel coating used in experiments described in the previous chapter dissolved in a wide range of organic solvents, but was durable in the ionic liquid used in the electrolyte developed by Wang *et al.*[2] Since nickel sheet, which is durable in an organic solvent solution, was to be used as the conducting substrate of the cathode in place of the commercial nickel formulation coated onto PET, the need to use an ionic liquid based electrolyte in the experiments described here was negated. As such, the electrolyte was switched to a formulation based on an organic solvent[3]. Further details of this electrolyte are included in the Experimental section of this chapter. .

3.1.1 Electrical Impedance Spectroscopy of Symmetric and Asymmetric cells

Electrical impedance spectroscopy (EIS) is an electrochemical characterisation method used to analyse circuit elements that exhibit complex, real world behaviour. These elements are too complicated to be analysed using the simple concepts of resistance and Ohm's Law. Instead, EIS is used to measure the ability of a circuit to resist the flow of an electrical current. Electrochemical impedance spectroscopy usually involves application of an AC potential to an electrochemical cell. The current passing through the cell is then measured. EIS has been widely used in the DSSC field to study the kinetics of electrochemical and photo-electrochemical processes occurring within a cell. [4-8].

The Nyquist plot is a method of presenting EIS data and is a parametric plot of the cell's frequency response. The Nyquist plot of a DSSC normally has three semicircles, representing the three main sources of resistance within the cell. These semicircles can be attributed to, in order of increasing frequency, Nernst diffusion within the electrolyte, electron transfer at the oxide/electrolyte interface at the working electrode and finally at the highest frequency, the redox reaction occurring at the counter electrode[2]. Any Nernst diffusion represented on EIS here describes only the diffusion of the triiodide ion in the electrolyte. Since a large excess of iodide ions in relation to triiodide ions exist in a typical DSSC electrolyte and the diffusion constants are of the same order of magnitude, the behaviour of the iodide ions does not contribute to the diffusion impedance detected here[9].

The aim of this set of experiments was to determine whether or not nickel coated with PEDOT-PTS is sufficiently stable, in comparable conditions, to be a viable alternative to the standard platinum coated FTO coated glass counter electrode most commonly used in DSSCs.

This study did not focus on the fabrication of many DSSCs for characterisation. Rather, specific and simplified cells were fabricated and electrochemically tested using EIS. This route was chosen to isolate the counter electrode/electrolyte electrochemical interactions and prevent grappling with possible complications associated with fabricating and testing full DSSCs. DSSCs have five main components so results from such cells would be much more complicated to elucidate, and results from complete cells could provide less useful information with respect to the counter electrode activity.

During this study, four different types of cells were investigated. All four cell variations contained one conventional DSSC cathode, i.e. platinum sputtered onto FTO coated glass. In addition, all four cell variations utilised the same electrode, which was based on the iodide/triiodide redox couple in MPN solvent [10]. The second electrode of each cell was varied. The four variations of the second electrode included in this study were:

1. A conventional DSSC cathode made from glass/FTO/sputtered platinum. This was described as a "symmetric cell".
2. FTO coated glass with a layer of PEDOT:PTS deposited on top. This cell was tested to determine if the replacement of platinum with PEDOT:PTS as the catalytic material resulted in a stable system, i.e. to isolate the change in the system when PEDOT:PTS was introduced.

3. *Nickel sheet sputtered with platinum.* This cell was tested to determine if replacement of FTO coated glass with nickel sheet resulted in a stable system, i.e. to isolate the change in the system when nickel was introduced.
4. Nickel sheet coated with a layer of PEDOT:PTS. This cell was tested to determine if the proposed alternate DSSC cathode, i.e. one fabricated from nickel and PEDOT:PTS. Results from this cell would serve to indicate whether or not incorporation of the Ni/PEDOT:PTS electrode would result in a stable system.

The cell variation described in (1) above, containing two conventional platinum/FTO coated glass DSSC cathodes, will be herein described as a symmetric cell as both electrodes are identical to each other. The other cells will be referred to according to the numbers and descriptions listed above. For example, “cell three” will describe a cell containing one standard DSSC cathode and one electrode made from nickel sheet sputtered with platinum.

3.1.2 Experimental

Platinized FTO coated glass electrodes were made using Solaronix TCO22-7 FTO (7 ohm resistivity) coated glass (Switzerland) that had been sputtered with 10 nm of platinum. Platinum deposition was performed at a chamber pressure of 10^{-7} mbar at ambient temperature. Nickel sheet (2 ohm resistivity) was sputtered with platinum to make cell three using the same conditions to produce the nickel/platinum electrode used to make cell three. PEDOT:PTS coated FTO coated glass electrodes were made using the vapour phase polymerisation technique described in the previous chapter. The oxidant solution was spin coated onto Solaronix TCO22-7 FTO coated glass using a Laurell Model WS-650SZ 6NPP/LITE/OND spin coater at 3000 rpm for 60 seconds. The remaining VPP process was carried out on the sample. After the VPP process was complete, approximately 150 nm of PEDOT:PTS had been deposited onto the FTO coated glass. This thickness was measured using a Dektak 6M profilometer. The PEDOT:PTS coated nickel electrode was fabricated using the same technique and conditions, the only change being that the FTO coated glass substrate used was replaced with a nickel sheet substrate. Profilometry confirmed that the same thickness of PEDOT:PTS of that deposited on the FTO coated glass had been deposited on the flexible nickel foil, i.e. approximately 150 nm.

Electrodes consisting of a nickel foil substrate were mounted onto glass to provide the rigidity required for cell fabrication. This step was required in this preliminary laboratory experiment, but could be easily eliminated as the research progressed. The two electrodes of each cell were sealed with a 25 micron thick Dupont Surlyn film (USA), which served as both an adhesive and a spacer

between the two electrodes. The cell was then filled with the electrolyte, which contained 0.8 M 1-propyl-3-methylimidazolium iodide, 0.15 M iodine, 0.1 M guanidinium thiocyanate and 0.5 M *N*-methylbenzimidazole in 3-methoxy propionitrile[2, 3].

Electrical impedance spectroscopy was used to assess the stability of the cells over a time period of seven days. Each cell was left physically connected to the apparatus for the entire seven day testing period, with no change in the electrical connections between the cell and the apparatus. This step was taken to avoid any changes in resistance stemming from inconsistencies in electrical connections over the testing period.

3.1.3 Results and Discussion

Figures 3.1 a – 3.1 d show Nyquist plots of impedance spectra of symmetric cells and the three variations of asymmetric cells over seven days using an I^-/I_2^- based electrolyte[2]. Figure 3.1 e shows the Legend that applies to all Nyquist plots.

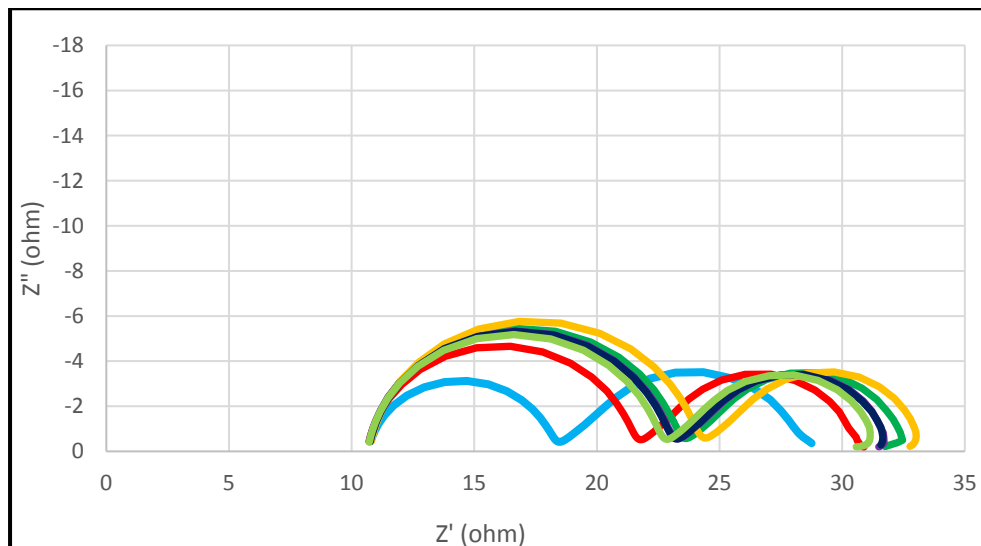


Figure 3.1 (a)

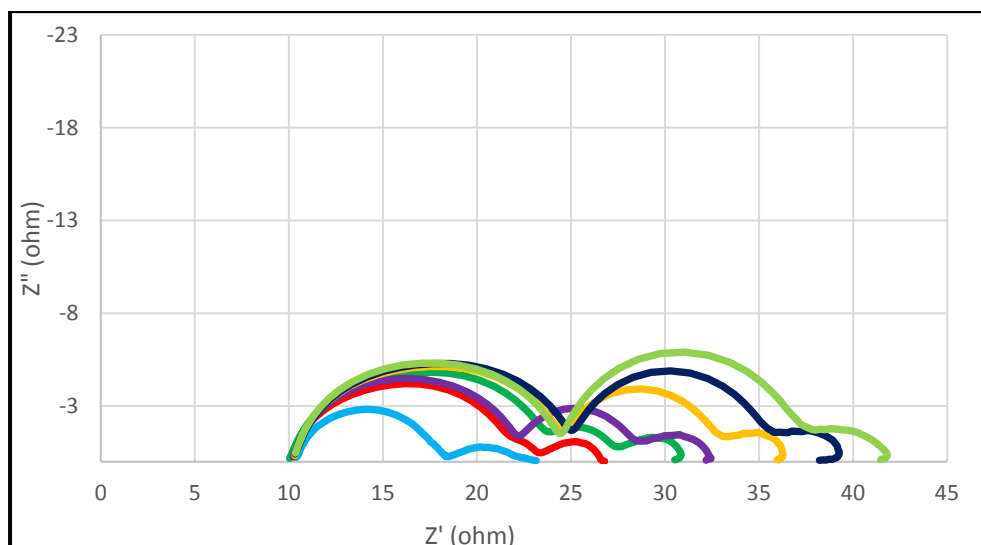


Figure 3.1 (b)

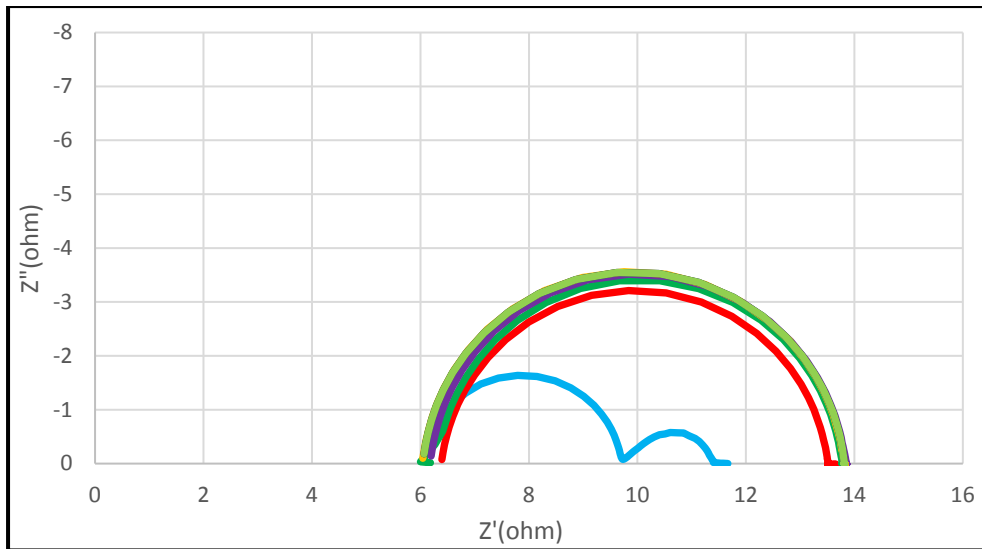


Figure 3.1 (c)

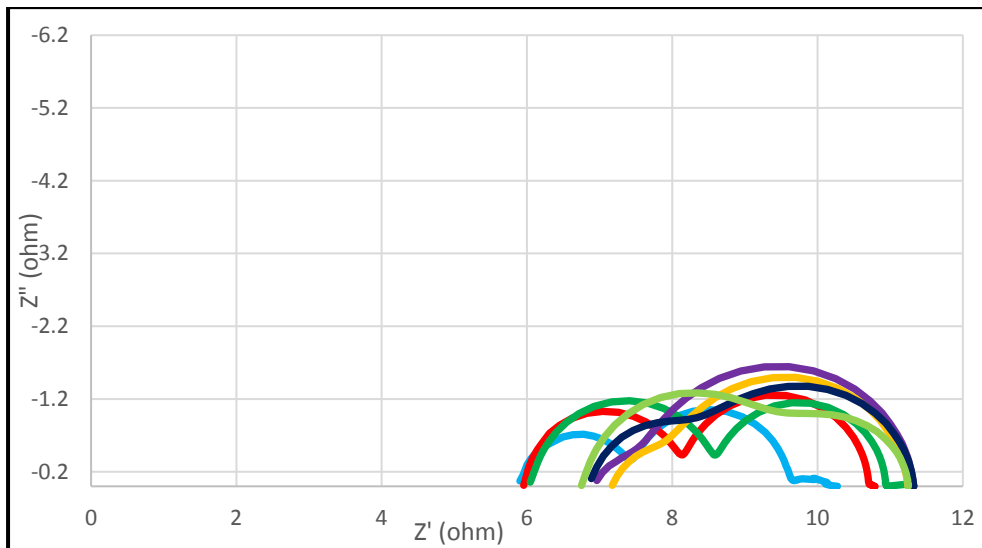


Figure 3.1 (d)



Figure 1. Nyquist plots of impedance spectra of symmetric cells and the three variations of asymmetric cells over seven days using an I^-/I_3^- based electrolyte[2] (a) symmetric FTO/Pt cell, I^-/I_3^- based electrolyte (cell 1) (b) asymmetric FTO/PEDOT-PTS and FTO/Pt cell (cell 2) (c) asymmetric Ni/Pt and FTO/Pt cell (cell 3) (d) Ni/PEDOT-PTS and FTO/Pt cell (cell 4).

The Nyquist plots of impedance spectra of the symmetric cells made using platinum sputtered FTO showed two semicircles only, representing the two primary contributing factors to the total impedance of the system.

EIS recorded from testing of the symmetric cell show the semicircle recorded at the higher frequency, with all seven spectra beginning at $Z' =$ between 10.7 and 10.8 Z' (ohm) can be attributed to the redox reaction occurring at the two identical electrodes. The semicircle recorded at the lower frequency, i.e. at $Z' = 18.4$ ohms after one hour and between 21.8 and 23.4 ohms during all subsequent spectra, represents the Nernst diffusion within the electrolyte[10]. Figure 3(a) shows that triiodide diffusion within the electrolyte is stable over the course of the experiment, which is to be expected in a stable electrolyte solution.

The Nyquist plot shown in Figure 3(a) indicates that the redox reaction occurring at the electrodes undergoes an equilibration period for approximately the first 24 hours, after which it stays relatively stable for the remaining six days in the experimental period. It is stated in the literature that there is some degradation of the platinum in a conventional DSSC electrode due to corrosion when an electrolyte based on the iodide/triiodide redox couple is used, as it is here[11, 12]. If this is correct, this equilibration period could, in fact, be due to platinum corrosion by the iodine species in the electrolyte. However, the starting point of each impedance spectrum recorded throughout the seven day testing period is constant and virtually identical at $Z' =$ between 10.7 and 10.8 Z' ohm for all seven spectra. This starting point is influenced by the resistance of wires making up the electrical connections, the resistance of the solder material connecting those wires to the cell and, finally, the sheet resistance of the electrode material. Since there was no change in electrical wires and connections over the experiment duration, the fact that this starting point is identical throughout the seven day period indicates that there is no change in the sheet resistance of the electrode material during the experiment. This can be extrapolated to theorise that there is no degradation of the platinum within the cell occurring. This cell can be considered stable over a seven day period.

The Nyquist plots of all three asymmetric cells showed three semicircles. This is to be expected considering each asymmetric cell comprises two different electrodes. The semicircles in each spectra can be attributed to Nernst diffusion within the electrolyte, electron transfer at the oxide/electrolyte interface at the working electrode and the redox reaction occurring at the counter electrode. In cases where only two, or even one, semicircle can be seen on the Nyquist plot, a large semicircle contained in the spectra has eclipsed one or two of the smaller semicircles so that they cannot be seen. In these cases, the system cannot be deconvoluted with any certainty.

The Nyquist impedance plots of cell 2, the asymmetric cells comprising a platinum sputtered FTO coated glass electrode and a PEDOT:PTS coated FTO coated glass electrode is depicted in Figure 1(b). The semicircle recorded at the highest frequency, beginning at between $Z' = 10.0$ and 10.4 ohms, can be attributed to the redox reaction occurring at the Pt/FTO/glass electrode/electrolyte interface. The centre semicircle, of which only a shoulder can be seen in the spectra recorded at 1 hour and 5 hours, can be attributed to electron transfer resistance at the PEDOT:PTS/FTO/glass electrode/electrolyte interface. The semicircle recorded at the lowest frequency results from Nernst diffusion of the triiodide ion within the electrolyte.

As seen in Figure 3(a), the redox reaction occurring at the counter electrode experienced an equilibration period over the first 24 hours of the experiment and then stayed relatively stable for the remaining time. Conversely, the size of the semicircle representing the activity at the PEDOT:PTS/FTO/glass electrode/electrolyte interface increases over the testing time, still not reaching stability after seven days. This is likely caused by swelling of the PEDOT:PTS coating with solvent of the electrolyte, i.e. 3-methoxypropionitrile (MPN). The swelling of PEDOT:PTS in solvent has been reported previously[13, 14] and it seems that swelling of PEDOT:PTS in MPN behaves similarly.

Experimental results of PEDOT:PTS swelling tests in MPN are reported later in this thesis.

In Figure 3(b), the semicircle attributed to Nernst diffusion within the electrolyte, i.e. the semicircle at the highest frequency, is not constant in size. This is consistent with the theory that PEDOT:PTS swells in MPN. If PEDOT:PTS absorbs the MPN solvent, MPN will be removed from the system as experiment time progresses and chemical equilibrium in the electrolyte will be disturbed. As a result, the diffusion rate of the ionic species within the electrolyte is not constant over the course of

the experiment. The swelling of PEDOT:PTS with MPN may also result in changes to the catalytic behaviour of PEDOT:PTS within the cell.

Again in Figure 3(b), the centre semicircle, representing electron transfer at the oxide/electrolyte interface at the working electrode, increases in size over the seven day experiment duration. This indicates that impedance (resistance) at the working electrode increases as time progresses in this system. This phenomenon is related to PEDOT:PTS swelling in MPN. Once swelling occurs, PEDOT:PTS no longer behaves in the same manner. This system is not stable over the seven day experimental period.

All spectra recorded over the seven day testing period for cell sample 3(b) begin at the same point on the Z' (ohm) axis, i.e. at between $Z'=10.0$ and 10.2 ohm. This indicates that there is no change in the sheet resistance of the electrode material during the experiment.

Figure 3(c), which shows results of EIS on cell three, shows Nyquist plots of impedance spectra of asymmetric cells made using an FTO coated glass electrode that had been sputtered with platinum and a nickel sheet electrode that had been sputtered with platinum. The first impedance spectra recorded during this experiment, i.e. the spectrum recorded after one hour, showed three semicircles. All subsequent spectra recorded after some time had passed showed only one semicircle.

After one hour, one, two or all three semicircles had increased in size to such a degree that only one semicircle is seen. The electrochemical interactions happening within the cell cannot be deconvoluted with any certainty from this spectra as the parameters, i.e. the size and position, of each semicircle cannot be discerned.

There is a very small change in the starting point of each spectra recorded for sample cell two throughout the seven day experiment duration, i.e. the spectra started at between $Z'=5.9$ and 6.4 ohm. Since all electrical connections remained constant throughout the experiment, this position change is indicative of some change in sheet resistance of the electrodes during the experiment. This will be discussed later on in this chapter.

The Nyquist plots of impedance spectra of the asymmetric cell fabricated using one standard DSSC counter electrode made from platinum sputtered FTO coated glass and one electrode made from

PEDOT-PTS coated nickel sheet are shown in Figure 3(d). Figure 3(d) shows three semicircles in the spectra recorded one hour, five hours and one day post cell fabrication. Subsequent spectra showed either only two semicircles, or one semicircle and a shoulder of a second semicircle.

As in Figure 3(c) the third component of the impedance spectra recorded after 24 hours and attributed to diffusion within the electrolyte had been eclipsed by the semicircles representing other impedance components. The sizes of all three semicircles, which each result from the different components of the cell the interface between the electrolyte and the PEDOT:PTS/Ni electrode, the interface between the electrolyte and the Pt/FTO/glass electrode and the Nernst diffusion within the electrolyte, either constantly change over the testing period of seven days or are eclipsed by the other semicircles in the spectra so that their actual size and positioning cannot be determined. As in Figure 3(b), this is likely caused in part by the swelling of PEDOT:PTS with MPN inside the cell, consequently affecting concentrations within the electrolyte and changing electrode | electrolyte interactions at both electrodes. A second contributing factor of the instability recorded in these spectra is likely to be the nickel electrode being corroded by iodine species contained in the electrolyte.

Similar to what is observed in Figure 3(c), the starting point of the impedance spectra in Figure 3(d), showing spectra of cell 4, is not stable over the seven day testing time. The spectra starting points in Figure 3(d) range from $Z'=5.7 - 7.1$ ohm. As previously mentioned, the nickel contained in the test electrodes in sample cells 3 and 4 is likely being corroded by the corrosive iodine containing electrolyte. The change in spectra starting point over the seven day experiment duration is much more pronounced in Figure 3(c) than 3(d), with the starting point changing $Z'=0.5$ ohm and $Z'=1.4$ ohm respectively. The sputtered platinum coating used in cell 3 seems to have a protective effect on the nickel. This protective effect has been previously reported in the literature [15]. It has been reported that a thin, continuous platinum layer sputtered onto the nickel sheet provides a protective physical barrier from the corrosive materials in the electrolyte. It appears that a certain amount of corrosion occurs, hence the small change in the electrical impedance spectra starting point, after which the surface is passivated and protected from any further degradation over the seven day experimental period.

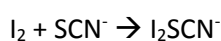
On the other hand, when considering sample cell 4, the comparatively larger variation in spectra starting point over the seven day period indicates that corrosion occurs to a larger extent here than in cell 3. This is to be expected since, during preparation of the experimental PEDOT:PTS coated

nickel counter electrode, the gravure printing of vapour phase polymerised PEDOT:PTS does not produce a continuous film on the nickel sheet surface. Hence, there is no effective physical barrier to protect the nickel metal from corrosive iodine species in the electrolyte. Furthermore, it is doubtful that the highly porous PEDOT:PTS could protect the nickel sheet from corrosion by the iodide/triiodide redox couple in the electrolyte since the porosity of the conducting polymer coating would enable the electrolyte to contact the nickel sheet.

The system represented in Figure 3(d), cell four, is the most unstable of all four systems. Not only is the nickel in the electrode susceptible to corrosion by iodine species in the electrolyte, but the protection provided by the sputtered Pt layer, such as that in cell 3 is absent. The results shown in Figure 3(d) indicate that PEDOT:PTS deposited through gravure printing and vapour phase polymerisation provides little to no protection against corrosion to the underlying nickel sheet contained in the electrode.

When considering the starting points of the first spectrum, recorded one hour after cell fabrication, of 3(a), 3(b), 3(c) and 3(d) at once, it is apparent that the two cells made using only glass/FTO electrode substrates (3(a) and 3(b)) had higher internal impedance than the two cells containing one glass/FTO electrode substrate and one nickel foil electrode substrate (3(c) and 3(d)). The starting points of the spectra in 3(a) and 3(b) are between $Z' = 10.0$ and 10.4 ohm, while the starting points of the spectra in 3(c) and 3(d) are between $Z' = 5.7$ and 7.1 ohm. This reflects the difference in starting surface resistivity of the glass/FTO substrate (7 ohm) and the nickel foil substrate (2 ohm). The difference in starting points between 3(a) and 3(b), even though both cells contain only FTO coated glass substrates which should have identical surface resistivity, can be explained by differences in the electrical connections between each cell and the testing apparatus. The same is true for the difference in starting points between 3(c) and 3(d).

It was observed that the electrolyte used to fabricate cells tested in this chapter underwent some degradation over time. When an aged solution of this electrolyte was used for electrochemical tests, i.e. when the solution had been formulated more than approximately two weeks previously, nonsensical and confusing results were obtained. This was possibly due to the thiocyanate anion in the electrolyte acting as a "pseudo halide" and coordinating with iodine over time, with the reaction proceeding as shown below. This reaction had been reported several times in the literature[16, 17].



The occurrence of this reaction would render some of the available iodine in the solution unavailable to the reaction system or alter the redox potential on the electrode. In turn, the concentrations of

the iodide and triiodide ions would decrease, leading to erratic results. To circumvent this issue for these tests, a fresh electrolyte solution was formulated each day. However, after the electrolyte is incorporated into a DSSC, this coordination reaction would still occur within the cell's electrolyte. Replacement of a cell's degraded electrolyte with fresh electrolyte after cell fabrication is unfeasible as it would be complicated and messy. Furthermore, it is possible that this type of electrolyte replacement could affect the other components of the DSSC. This electrolyte phenomenon signifies that, regardless of any counter electrode/electrolyte interactions discussed in this chapter, DSSC performance of a cell using the electrolyte used here, would not be expected to be stable over a period of greater than two weeks.

3.1.4 Conclusion

Through analysing data from EIS experiments performed on asymmetric cells containing a conventional glass/FTO/platinum electrode and an alternate nickel sheet/PEDOT:PTS electrode, the likeliness of degradation of the nickel, by means of corrosion, by the iodide/triiodide redox couple in the electrolyte was established. Corrosion was suspected as there was obvious instability in the cells containing nickel foil as a conducting electrolyte substrate. In the cell that contained a nickel sheet electrode that was not protected by a sputtered platinum layer, this instability was further pronounced.

Further instability within cells containing the PEDOT:PTS catalytic layer was present due to the PEDOT:PTS swelling with the electrolyte solvent, MPN. This phenomenon may result in changing the catalytic behaviour of PEDOT:PTS and causing inconsistencies in concentrations within the electrolyte by disturbing the chemical equilibrium of the solution.

Furthermore the thiocyanate in the electrolyte appears to be coordinating with electrolyte iodine over time, causing changes in the concentration of iodine species in the electrolyte. These two factors, i.e. corrosion and iodine species ion coordination, serve to render the system unstable, indicating that the nickel/PEDOT counter electrode and an electrolyte based on the iodide/triiodide redox couple are unsuitable for use together in a DSSC. In fact, since the coordination of thiocyanate anions with iodine species is a reaction that occurs within the electrolyte itself, this electrolyte is unsuitable for long term use within a DSSC.

Further testing on this system will be presented in the next chapter.

Chapter 3 References

1. Wang, P., et al., *A binary ionic liquid electrolyte to achieve $\geq 7\%$ power conversion efficiencies in dye-sensitized solar cells*. Chemistry of Materials, 2004. **16**(14): p. 2694-2696.

2. Wang, Q., J.E. Moser, and M. Gratzel, *Electrochemical impedance spectroscopic analysis of dye-sensitized solar cells*. Journal of Physical Chemistry B, 2005. **109**(31): p. 14945-14953.
3. Wang, P., et al., *Stable >= 8% efficient nanocrystalline dye-sensitized solar cell based on an electrolyte of low volatility*. Applied Physics Letters, 2005. **86**(12): p. 3.
4. Kern, R., et al., *Modeling and interpretation of electrical impedance spectra of dye solar cells operated under open-circuit conditions*. Electrochimica Acta, 2002. **47**(26): p. 4213-4225.
5. Kim, Y.K., et al., *Impedance spectroscopy on dye-sensitized solar cells with a poly(ethylenedioxythiophene):poly(styrenesulfonate) counter electrolyte*. Journal of the Korean Physical Society. **60**(12): p. 2049-2053.
6. Han, L.Y., et al., *Modeling of an equivalent circuit for dye-sensitized solar cells*. Applied Physics Letters, 2004. **84**(13): p. 2433-2435.
7. Hoshikawa, T., et al., *Impedance analysis of internal resistance affecting the photoelectrochemical performance of dye-sensitized solar cells*. Journal of the Electrochemical Society, 2005. **152**(2): p. E68-E73.
8. Fabregat-Santiago, F., et al., *Influence of electrolyte in transport and recombination in dye-sensitized solar cells studied by impedance spectroscopy*. Solar Energy Materials and Solar Cells, 2005. **87**(1-4): p. 117-131.
9. Hauch, A. and A. Georg, *Diffusion in the electrolyte and charge-transfer reaction at the platinum electrode in dye-sensitized solar cells*. Electrochimica Acta, 2001. **46**(22): p. 3457-3466.
10. Hoshikawa, T., et al., *Effects of electrolyte in dye-sensitized solar cells and evaluation by impedance spectroscopy*. Electrochimica Acta, 2006. **51**(25): p. 5286-5294.
11. Syrokostas, G., et al., *Degradation mechanisms of Pt counter electrodes for dye sensitized solar cells*. Solar Energy Materials and Solar Cells, 2012. **103**: p. 119-127.
12. Olsen, E., G. Hagen, and S.E. Lindquist, *Dissolution of platinum in methoxy propionitrile containing LiI/I₂*. Solar Energy Materials and Solar Cells, 2000. **63**(3): p. 267-273.
13. Sirimanne, P.M., et al., *Towards an all-polymer cathode for dye sensitized photovoltaic cells*. Thin Solid Films. **518**(10): p. 2871-2875.
14. Armel, V., et al., *Unexpected Interaction between PEDOT and Phosphonium Ionic Liquids*. Journal of the American Chemical Society. **135**(30): p. 11309-11313.
15. Miettunen, K., et al., *Stabilization of metal counter electrodes for dye solar cells*. Journal of Electroanalytical Chemistry. **653**(1-2): p. 93-99.
16. Long, C. and D.A. Skoog, *A THIOCYANATE COMPLEX OF IODINE(I)*. Inorganic Chemistry, 1966. **5**(2): p. 206-&.
17. Wood, C.J., C.A. McGregor, and E.A. Gibson, *Does Iodine or Thiocyanate Play a Role in p-Type Dye-Sensitized Solar Cells?* Chemelectrochem, 2016. **3**(11): p. 1827-1836.

Chapter 4: Additional testing of the system containing nickel/PEDOT:PTS electrode and iodine based electrolyte.

4.1 Introduction

Tests, in addition to the electrical impedance spectroscopy discussed in Chapter 3, were conducted on cells containing a nickel/PEDOT:PTS electrode and the organic solvent electrode containing the iodide/triiodide redox couple. This additional testing included:

1. Further electrochemical analysis of the system: Tafel plots
2. Wet chemistry testing to confirm presence of nickel in iodine based electrolyte.
3. Swelling of PEDOT:PTS in methoxypropionitrile (MPN) solvent.

These additional tests are discussed in this chapter. Tests 1 and 2 were conducted to conclusively determine if corrosion was occurring within the proposed DSSC system containing nickel and the iodide/triiodide redox couple. Test 3 was conducted to determine if swelling of the PEDOT:PTS polymer coating comprising part of the electrode was swelling in the electrolyte solvent, and if that could explain the instability noted in Chapter 3, Figure 3 (b).

4.2 Further electrochemical analysis of the system: Tafel plots

Since corrosion was assumed to be present in the cells described in Chapter 3, which contained a Ni/PEDOT:PTS electrode and an iodine based electrolyte[1], further electrochemical studies were carried out on the system. Electrochemical studies are ideal to use to study corrosion as corrosion occurs via electrochemical reactions. Here, data was collected to construct Tafel plots to describe electrochemical behaviour of the system.

Tafel plots can aid in understanding the corrosion behaviour of a system by revealing the equilibrium that exists between two opposing chemical reactions. One of these reactions is an anodic reaction, a metal (in this case nickel) is being oxidised. The opposing reaction is a cathodic reaction, a solution species (in this case I⁻) is reduced. When these two reactions are in equilibrium, the flow of electrons from each reaction is balanced and no net electron flow, or external electric current, is present. Tafel plots represent this process; the x axis is the electric potential and the y axis is the logarithm of the absolute value of current. The sharp minimum in the curve is the point where the current reverses polarity as the reaction changes from anodic or cathodic and is caused by using a logarithmic axis. A logarithmic axis is required due to the wide range of current values that are commonly recorded during a corrosion experiment. Because of the phenomenon of passivity, the measured current can change by six orders of magnitude during a corrosion experiment[2].

Before carrying out cyclic voltammetry experiments generating data to construct Tafel plots, a conversion factor needed to be determined experimentally to accommodate the use of the non-

standard platinum reference electrode in the experiment. This conversion factor allows for the experimental redox potential of the iodide/triiodide redox reaction, determined through cyclic voltammetry experiments, to be compared to a theoretical redox potential for the same reaction. The ferrocenium/ferrocene redox couple has often been used as an internal standard for reporting electrode potentials due to the assumption that the redox potential of this couple remains approximately constant, regardless of the solvent. The ferrocenium/ferrocene redox couple was used here[3].

4.2.1 Experimental

To experimentally determine the conversion factor required to compensate for using a non-standard platinum reference electrode, cyclic voltammetry experiments were run using a system employing the ferrocenium/ferrocene redox couple as an internal standard. Cyclic voltammetry for this analysis was carried out using a multi-channel potentiostat controlled using VMP2 EC-lab 9.56 software. For this experiment, an electrolyte similar to the MPN/iodine redox couple electrolyte used previously[4] was made up. In this electrolyte however, the iodide/triiodide was replaced with ferrocene. The electrolyte used here was comprised of 1 mM ferrocene (TNJ, China), 0.5 M NMBI (TCI Chemicals, Japan) and, to enable conductivity, a small amount of tetrabutylammonium hexafluorophosphate (Sigma Aldrich, Australia) in MPN (Dow, USA). The three electrode cell used in this experiment consisted of a platinum wire working electrode (0.5 mm thick, Sigma Aldrich, Australia) a titanium mesh counter electrode (Biomedent, Singapore) and an Ag/Ag⁺ standard electrode made from MPN and silver nitrate (Alfa Aesar, USA). Cyclic voltammetry sweeps of the system were taken at three different scan rates, i.e. 5, 20 and 200 mV s⁻¹.

Cyclic voltammetry carried out to construct Tafel plots for this analysis was carried out using the same potentiostat and software listed above. Two similar cells were tested during this experiment. Both cells employed a platinum wire used as both the counter and reference electrode and a typical iodide/triiodide organic solvent based DSSC electrolyte[5]. The electrolyte contained 0.8 M 1-propyl-3-methylimidazolium iodide, 0.15 M I₂I₂, 0.1 M guanidinium thiocyanate, and 0.5 M NN-methylbenzimidazole in MPN. The two cells differed in that one cell, Cell A, used a nickel electrode as the working electrode and the other cell, Cell B, used a PEDOT:PTS coated nickel electrode as the working electrode. The nickel electrode used in Cell B was coated with PEDOT:PTS using the gravure printing and vapour phase PEDOT:PTS polymerisation method outlined in Chapter 2. Both working electrodes consisted of 1.0 cm x 2.0 cm pieces of nickel foil 0.125 mm thick (Sigma Aldrich, Australia). The platinum wire for the working and reference electrodes was 0.5 mm thick (Sigma Aldrich, Australia).

The cells were connected to the potentiostat and allowed to equilibrate to determine their open circuit potential (V_{oc}). This open circuit potential was used to determine the potential range of the

sweeps to be carried out.

A controlled potential was applied to the cell to mimic the conditions a working DSSC would be under during operation. The cell was subjected to a sweep between 0.2 V and -0.2 V at a very slow scan rate of 0.166 mV/s with a three hour rest period between scans. The scans were run until no further change to the results was observed with respect to both Cell A and Cell B.

4.2.2 Results and Discussion

Figure 4.1 depicts the cyclic voltammograms of the Pt working electrode described in 4.1.2.

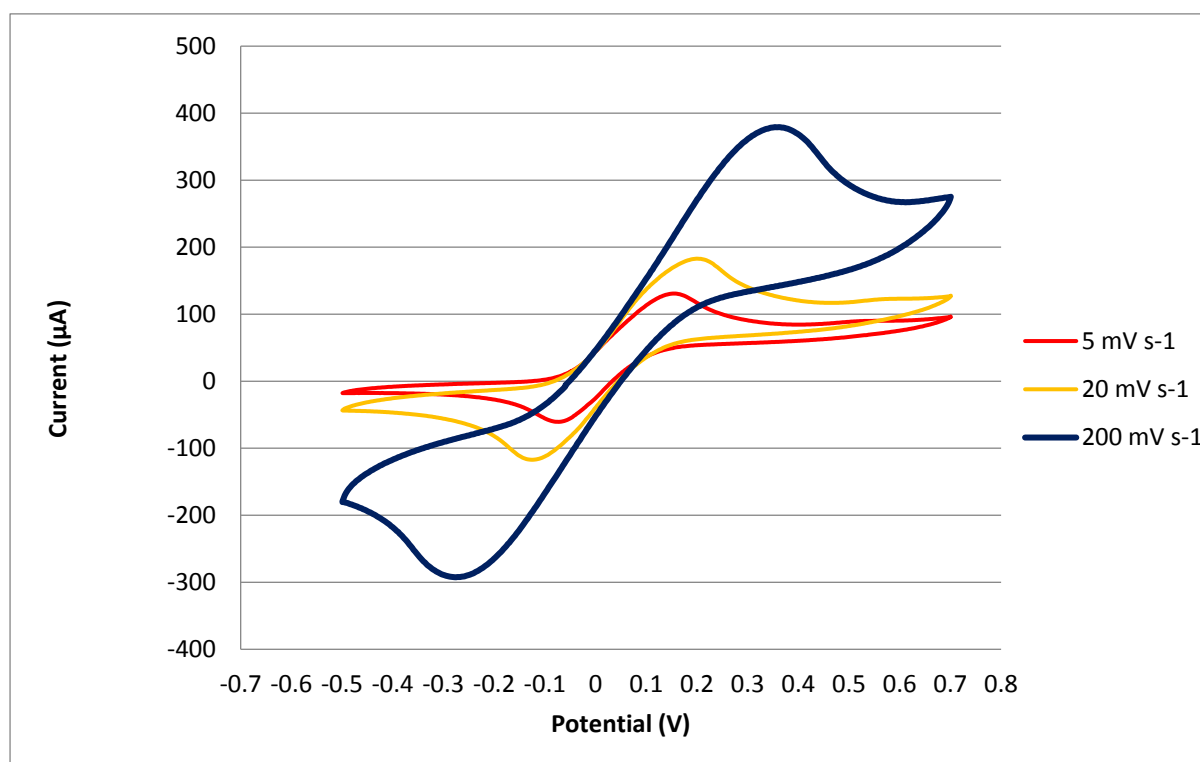


Figure 4.1: Cyclic voltammograms of Pt working electrode described in 4.2.2 using scan rates of five, 20 and 200 mV s⁻¹.

To calculate the conversion factor from these experimental results, the average central point of the three scans of ferrocene in Figure 4.1 was determined. This was found to be 0.041 V +/- 0.003 V. As such, the potential of the platinum working electrode vs the Ag/Ag⁺ electrode was found to be -0.028 V. From this experimental value, literature values for conversion constants for redox potentials measured versus the standard hydrogen electrode (SHE) in acetonitrile solutions were used to determine the expected redox potential of the iodide/triiodide system that was to be investigated. The assumption was made that the electrochemical behaviour of the system in the MPN solution used would be similar to the behaviour if an acetonitrile solution was employed. The conversion constant was calculated as follows:

To convert from the SHE to an Ag/Ag⁺ electrode in an acetonitrile solvent, 0.601 V must be added[6]. To convert from an Ag/Ag⁺ electrode in acetonitrile to the Pt electrode in this experiment, -0.028 V

must be added (determined experimentally).

Hence, the conversion factor required is 0.629 V.

Before conducting scans to construct Tafel plots, the open circuit potential was determined to ascertain the potential range of the sweep to be carried out. The V_{oc} of both cells was found to be -0.065 V.

A very slow scan rate of 0.166 mV/s was used with a three hour rest period between scans. This slow scan rate was selected to prevent the steady state reaction conditions at the metal surface from being disturbed[7], i.e. to mimic the true behaviour of the system containing the nickel/PEDOT:PTS electrode and iodide/triiodide based electrolyte inside a DSSC.

Figures 4.2 and 4.3 depict Tafel plots of corrosion experiment results employing a nickel working electrode and a nickel/PEDOT:PTS working electrode respectively.

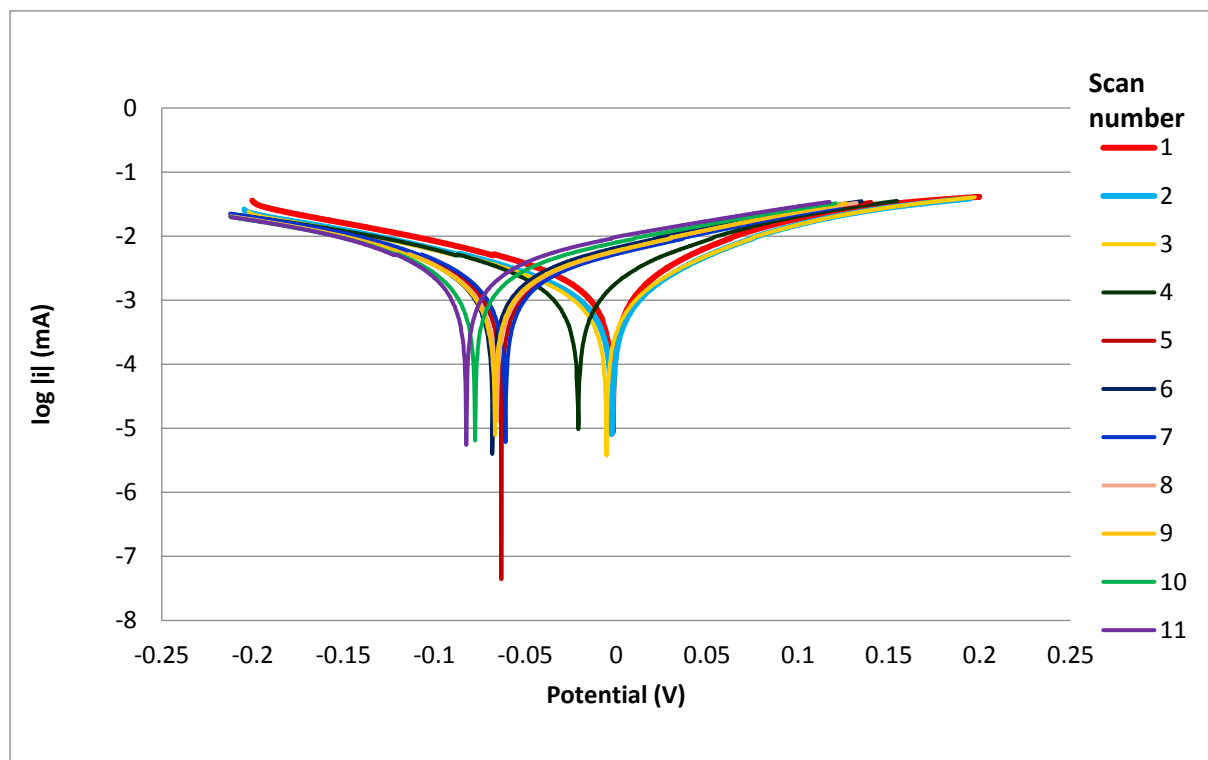


Figure 4.2: Tafel plot of corrosion experiment results employing a nickel working electrode, a titanium mesh counter electrode, a platinum reference electrode and an iodide/triiodide based electrolyte[8]. The potentials on this plot are referenced to a platinum reference electrode.

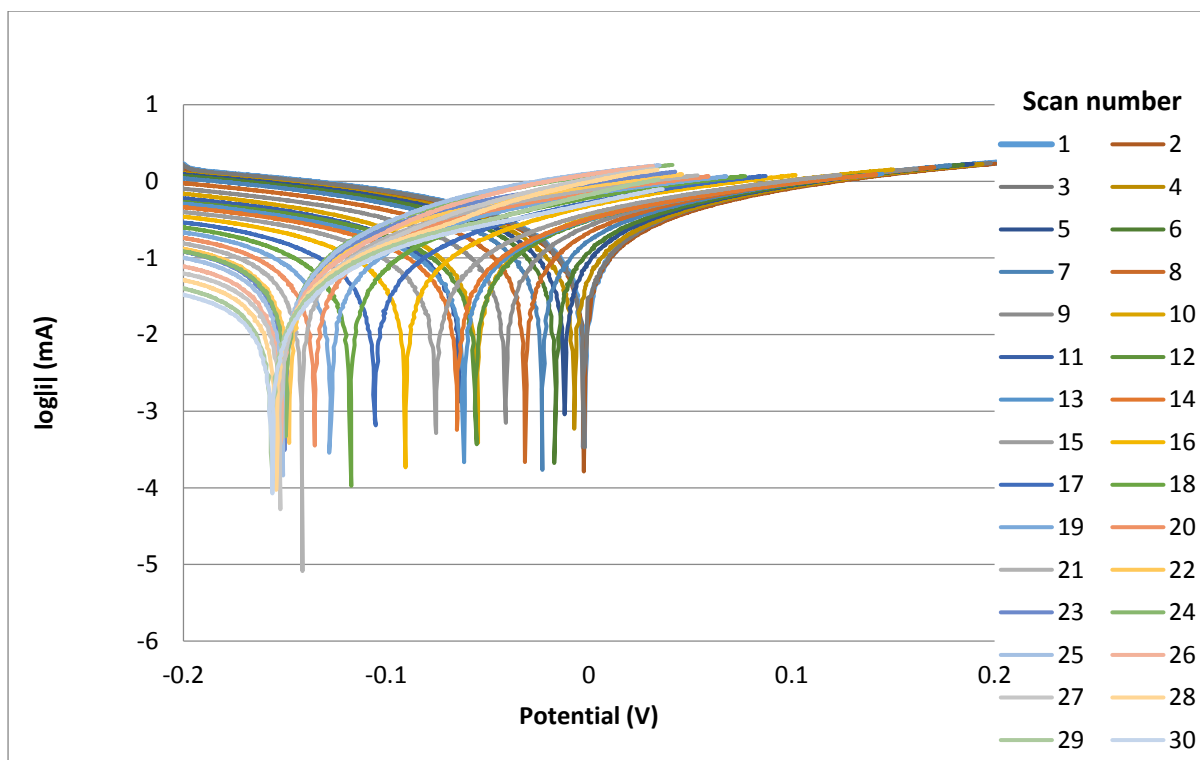


Figure 4.3: Tafel plot of corrosion experiment results employing a nickel/PEDOT:PTS working electrode, a titanium mesh counter electrode, a platinum reference electrode and an iodide/triiodide based electrolyte[8]. These potentials on this plot are referenced to a platinum electrode.

The calculated reduction potential of the iodide/triiodide redox reaction in this system is -0.093 V vs platinum. This is the standard reduction potential of the reaction, referenced to a SHE, after application of the conversion factor. This reduction potential corresponds to the minimum from the first sweep in Figure 4.2, indicating that the conventional iodide/triiodide redox reaction is taking place at this early stage of the reaction. Subsequently, during sweeps 2, 3 and 4, there is a shift towards $0.02 - 0$ V. After this point, the remaining sweeps show minimums, again, around -0.09 to -0.1 V. The converted standard redox potential of nickel in this system is expected to be 0.17 V. Although this value does not correspond to the peaks resulting from sweeps 2 to 4, i.e. around $0.02 - 0$ V, the location of the peaks could be resulting from nickel corrosion occurring in tandem with the iodide/triiodide redox reaction. After sweep 4, the results indicate that the nickel has been passivated. As such, corrosion of nickel is no longer occurring and the peak is again corresponding to the iodide/triiodide redox reaction. From Figure 4.2, it appears that the nickel electrode takes the time of four scans to become passivated; this corresponds to between 14 – 15 hours.

The first peak in Figure 4.3, like Figure 4.2, corresponds to the reduction potential of the iodide/triiodide redox reaction. After this time, peaks from sweeps 2, 3 and 4 are again close to 0 V. However, in Figure 4.3 they are between 0 and 0.01 V. After this time, the location of the peaks

moved gradually from approximately 0.01 V to -0.15 V. The time required for the electrochemical behaviour to stabilise in this system was the time required for 22 scans to be run. This corresponds to a total time of 80 hours and 40 minutes, or three days and eight hours.

4.3 Wet chemistry testing to confirm the presence of nickel in iodine based electrolytes.

4.3.1 Experimental

Two tests, very similar to each other, were set up to confirm the occurrence of nickel corrosion in an iodide/triiodide DSSC electrolyte. Two nickel foil samples (0.125 mm thick, Aldrich, Australia) were placed into separate vials containing a typical iodide/triiodide DSSC electrolyte that incorporated an MPN solvent (Dow, USA)[8]. One of the nickel foil samples was immersed in the electrolyte in its original state. PEDOT:PTS was bar coated on the second nickel foil sample using a RK Print Meter Bar Coater and the vapour phase polymerisation technique first outlined in Chapter 2. This second, PEDOT:PTS coated nickel foil sample was then immersed in the electrolyte. The vials were then left undisturbed under ambient conditions for 72 hours. The nickel foil pieces were removed from solution after 72 hours and the solutions were filtered and tested for both iodine and nickel.

The precipitate from each vial was tested for nickel by first dissolving a small amount in dilute ammonia solution (0.1 M, Merck, Germany). A few drops of 1% dimethylglyoxime ethanol solution (LabChem, USA) was added (Sigma Aldrich, Australia) to the solution containing the dissolved precipitate and the solution was agitated by hand to mix.

The precipitate from each vial was then tested for iodine to determine if the concentration of iodine, and as a result the concentrations of iodide and triiodide, was impacted by the corrosion activity associated with the nickel foil being immersed in the electrolyte solution.

To test for iodine, a small amount of the original precipitate was dissolved in solution – this time in dilute nitric acid (Sigma Aldrich, Australia). Dilute nitric acid was used as the solvent here because nitric acid will react with, and remove, other ions that may react with silver nitrate to form a precipitate. This reduces the chances of obtaining confusing results that require deconvolution. An 0.5 M aqueous solution of silver nitrate (Alfa Aesar, USA) was added to the nitric acid/original precipitate solution and a cream coloured precipitate (silver iodide) was formed, indicating the presence of iodine in the original precipitate. Since other halide anions, i.e. chloride and bromide, also form a precipitate with silver cations, the precipitate was confirmed to be silver iodide using ammonia solution (Merck, Germany). Silver chloride, silver bromide and silver iodide all have differing solubilities in ammonia solution; silver chloride is soluble in dilute ammonia solution, silver bromide is insoluble in dilute ammonia solution but soluble in concentrated ammonia solution and silver iodide is insoluble in ammonia solution of any concentration. The precipitate was mixed with concentrated ammonia solution and found to be insoluble, thus confirming this silver halide salt to

be silver iodide.

4.3.2 Results and Discussion

There was a visible colour change to the electrolyte after the electrodes were immersed for 72 hours. Images of the vials are shown in Figure 4.4 and Figure 4.5.

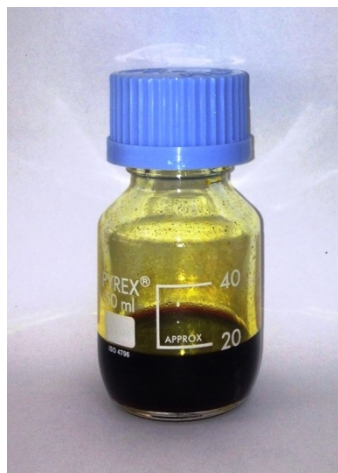


Figure 4.4: Initial electrolyte colour

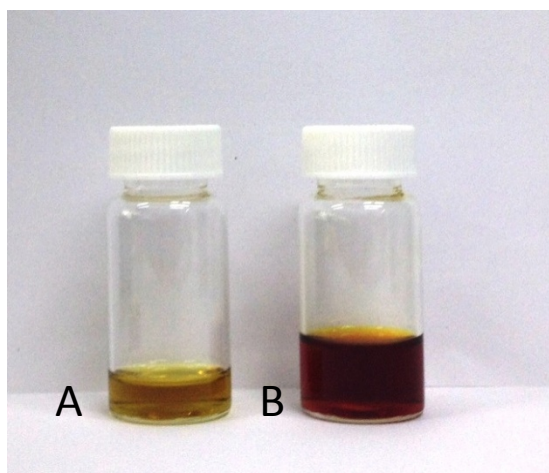
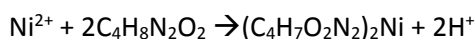


Figure 4.5 (A) Electrolyte colour after nickel/PEDOT:PTS electrode immersion and (B) electrolyte colour after nickel electrode immersion.

24 hours after the initial experiment set up, an abundance of precipitate was observed in the vial containing nickel foil coated with PEDOT:PTS. There was a comparatively small amount of precipitate in the vial containing the uncoated nickel foil.

72 hours after the initial experiment set up, the vials appeared to contain approximately the same amount of precipitate. The precipitate from each vial was tested for both nickel and iodine as a means to confirm corrosion was occurring. If corrosion was definitely occurring within either system, there would be both nickel and iodine present in the precipitate from each reaction vial. A fine pink precipitate was formed from both solutions made by dissolving the original precipitate

when this test was carried out, confirming the presence of nickel in the precipitate. This pink precipitate is nickel dimethylglyoxime. The reaction proceeded according to the following reaction:



The precipitate from each vial was tested for iodine using a well-known precipitation reaction between $\text{Ag}^+_{(\text{aq})}$ and $\text{I}^-_{(\text{aq})}$ was employed[9] to test for the presence of iodine in the precipitate. The presence of iodine was confirmed.

The nickel that was proven to be present in the precipitate originated from the nickel foil samples that had been immersed in the electrolyte, confirming that nickel corrosion was occurring. It was anecdotally observed that precipitate was produced at a faster rate in the vial containing nickel foil that had been coated with PEDOT:PTS than the vial containing uncoated nickel foil. This indicates that the presence of PEDOT:PTS hastened the reaction of nickel with the iodine species in the electrolyte solution, i.e. corrosion.

4.4 Swelling of PEDOT:PTS in methoxypropionitrile.

There have been reports of poly (3,4-ethylenedioxythiophene) polystyrene sulfonate (PEDOT:PSS) swelling in organic solvent[10-12]. These reports describe the swelling of PEDOT:PSS in glycerol (Snaith *et al.*, 2005) and DMSO (Dimitriev *et al.*, 2009) and the swelling of PEDOT:PTS in water. All three reports described a marked increase in PEDOT:PSS conductivity with swelling. When PEDOT:PSS was deposited using solution processing from aqueous solution as a colloidal dispersion with excess polystyrene sulfonate present, this conductivity increase was caused by greater aggregation of the PEDOT-rich colloidal particles occurring during swelling. Snaith *et al.* reported a conductivity increase of three orders of magnitude with the addition of glycerol, i.e. swelling of the PEDOT:PSS polymer with glycerol. Winther-Jensen *et al.*[12] used a vapour phase polymerisation technique to produce PEDOT:PTS, similar to the VPP used in the experiments described in Chapters 2 and 3. Winther-Jensen *et al.*'s study was focussed on catalytic activity of PEDOT:PTS for hydrogen generation. In this case, the measured water uptake of the PEDOT coating over 24 hours was 26% and the measured catalytic activity of PEDOT:PTS increased after swelling with glycerol.

Here, the percentage mass of MPN absorbed by a PEDOT:PTS film, and the absorption rate of MPN, was determined in order to gauge the magnitude of impact this phenomenon would have on the system within a DSSC.

4.4.1 Experimental

To quantify the mass of MPN absorbed by a PEDOT:PTS film over time, A QCM200 Quartz Crystal Microbalance was used in conjunction with the Sauerbrey equation[13]. This process was described in more detail in Chapter 2.

PEDOT:PTS was deposited onto a quartz crystal resonator using spin coating and subsequent vapour

phase polymerisation, as described in Chapter Two. The VPP oxidant was first spin coated onto the quartz crystal resonator at a speed of 3000 rpm for 60 seconds using a Laurell WS-650-23B spin coater. The VPP process followed to yield a thin film of PEDOT:PTS. This PEDOT:PTS coated quartz crystal resonator was placed inside a crystal holder filled with methoxypropionitrile solvent (>98%, Sigma Aldrich, Australia). The MPN film is referred to a platinum reference electrode. The resonance frequency of the quartz crystal microbalance was recorded over a period of 35 days. From this information, the mass change of the deposited PEDOT:PTS film over that time was calculated using the Sauerbrey equation.

4.4.2 Results and Discussion

The mass change in the film over the testing period of 35 days is shown in the Figure 4.6.

The mass of the film percentage increase first decreases sharply between the testing times of zero days and one day, from 8.1 to 4.6%. It then increases between the testing time of one day and nine days to a maximum of 12.1 mass percentage increase. Between nine days and 26 days, the film mass steadily falls and then remains virtually constant at approximately 9% mass percentage increase for the remainder of the testing time.

It is possible that a small amount of residual ethanol, from rinsing, was incorporated into the PEDOT:PTS film at the commencement of this testing. The release of this residual ethanol would account for the initial decrease in mass over the first day of testing. The decrease in the film mass between day nine and day 26 may have been due to a portion of the MPN associated with the PEDOT:PTS film not being truly incorporated into the polymeric framework. If some of the MPN was simply adsorbed onto the surface of the film, this MPN may have been subsequently liberated, causing the mass loss observed.

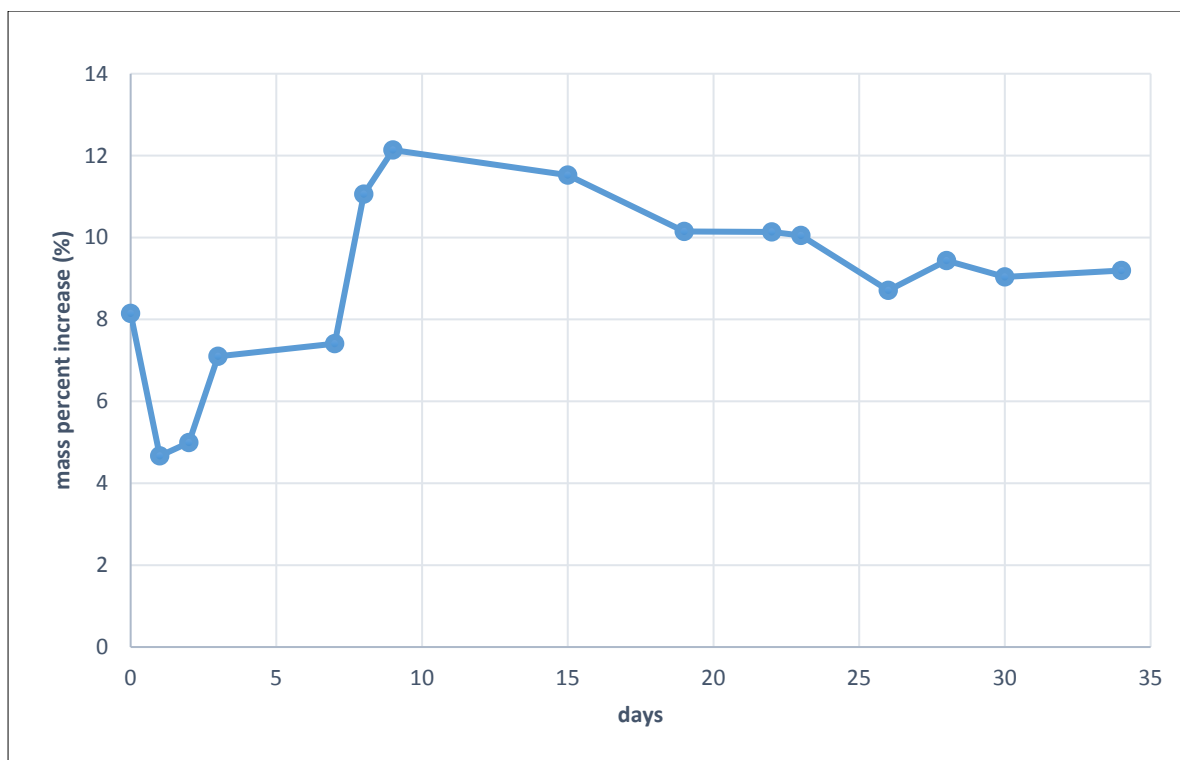


Figure 4.6: Chart showing time elapsed versus PEDOT:PTS mass increase due to MPN swelling.

It is important to note that, during this experiment, VPP PEDOT:PTS was deposited using spin coating instead of gravure printing. It was not possible to use the quartz crystal resonator as a substrate for gravure printing due to the size of the resonator and the gravure printing apparatus available. The possible implications of using spin coating as the deposition method, rather than gravure printing, centre around inherent morphology differences in films deposited using the two very different deposition methods. During spin coating deposition, the deposited film dries while under centrifugal force due to the rapidly spinning chuck. In contrast, when a material is gravure printed, it does not experience this centrifugal force and is instead subjected to substrate wettability and internal surface tension forces. For this reason, film morphology will likely be different in films that are spin coated to those that have been printed.

4.5 Conclusion

Through the electrochemical tests detailed in sections 4.3 and 4.4, corrosion of the nickel electrode by the iodine species in the DSSC was confirmed. This was surprising since, in 2004, Ma *et al.* reported a successful study on the use of a counter electrode with a nickel metal substrate in conjunction with an iodide/triiodide based electrolyte[14]. This study included stability tests on nickel in the iodide/triiodide electrolyte solution; good stability was of nickel sheet in the electrolyte solution for three months was reported.

For an electrode of this type to be a viable proposition for use in DSSC commercialisation, an electrolyte employing a redox couple other than the iodide/triiodide redox couple must be used.

This is explored in the next chapter.

The swelling test described in section 4.4 shows that a spin coated PEDOT:PTS film absorbs a maximum of about 12 % MPN when immersed in the solvent, with equilibrium between the solvent and the film reached after 26 days. This can be extrapolated to an expectation that a DSSC electrode employing gravure printed PEDOT:PTS will reach stability with respect to this particular PEDOT:PTS/electrolyte interaction 26 days post fabrication.

Chapter 4 References

1. Wang, P., et al., *Stable >= 8% efficient nanocrystalline dye-sensitized solar cell based on an electrolyte of low volatility*. Applied Physics Letters, 2005. **86**(12).
2. Gamry *Basics of Electrochemical Corrosion Measurements*. Available from: <https://www.gamry.com/application-notes/corrosion-coatings/basics-of-electrochemical-corrosion-measurements/>.
3. Fox, D.M., et al., *Flammability, thermal stability, and phase change characteristics of several trialkylimidazolium salts*. Green Chemistry, 2003. **5**(6): p. 724-727.
4. Awadhia, A. and S.L. Agrawal, *Structural, thermal and electrical characterizations of PVA : DMSO : NH4SCN gel electrolytes*. Solid State Ionics, 2007. **178**(13-14): p. 951-958.
5. Wang, P., et al., *Stable >= 8% efficient nanocrystalline dye-sensitized solar cell based on an electrolyte of low volatility*. Applied Physics Letters, 2005. **86**(12): p. 3.
6. Isse, A.A. and A. Gennaro, *Absolute Potential of the Standard Hydrogen Electrode and the Problem of Interconversion of Potentials in Different Solvents*. Journal of Physical Chemistry B, 2010. **114**(23): p. 7894-7899.
7. Baboian, R., *Corrosion Tests and Standards*. 2004 ed. 2004.
8. Wang, Q., J.E. Moser, and M. Gratzel, *Electrochemical impedance spectroscopic analysis of dye-sensitized solar cells*. Journal of Physical Chemistry B, 2005. **109**(31): p. 14945-14953.
9. *Testing for halide ions*; www.chemguide.com.uk.
10. Dimitriev, O.P., et al., *PEDOT:PSS films-Effect of organic solvent additives and annealing on the film conductivity*. Synthetic Metals, 2009. **159**(21-22): p. 2237-2239.
11. Snaith, H.J., et al., *Morphological and electronic consequences of modifications to the polymer anode 'PEDOT : PSS'*. Polymer, 2005. **46**(8): p. 2573-2578.
12. Winther-Jensen, B., et al., *Conducting Polymer Composite Materials for Hydrogen Generation*. Advanced Materials, 2010. **22**(15): p. 1727-+.
13. Sauerbrey, G., *VERWENDUNG VON SCHWINGQUARZEN ZUR WAGUNG DUNNER SCHICHTEN UND ZUR MIKROWAGUNG*. Zeitschrift Fur Physik, 1959. **155**(2): p. 206-222.
14. Ma, T.L., et al., *Properties of several types of novel counter electrodes for dye-sensitized solar cells*. Journal of Electroanalytical Chemistry, 2004. **574**(1): p. 77-83.

Chapter 5: EIS of a cell containing the nickel/PEDOT:PTS electrode and an electrolyte containing the cobalt^{II/III} redox couple.

5.1 Introduction

Through experiments described in Chapters 3 and 4, it was determined conclusively that a nickel based electrode and an electrolyte containing the iodide/triiodide based redox couple are incompatible for use together in a DSSC. This is because the corrosive iodide/triiodide redox couple will degrade the nickel in the electrode. A preliminary investigation was conducted here into the compatibility of a nickel based electrode with an electrolyte using an alternate redox couple to the iodide/triiodide redox couple. This was done to indicate if the Ni/PEDOT:PTS electrode would be compatible with any type of DSSC electrolyte. An electrolyte containing the cobalt^(II/III) redox couple was used in this investigation. EIS data was recorded over a seven day period to assess the stability of the system.

5.1.1 Experimental

Cells were fabricated using one standard glass/FTO/Pt electrode and one Ni/PEDOT:PTS electrode. Platinized FTO coated glass electrodes were made from Solaronix TCO22-7 FTO coated glass (Switzerland) that had been sputtered with 10 nm of platinum. The platinum deposition was carried out at a chamber pressure of 10^{-7} mbar and ambient temperature. The PEDOT:PTS coated nickel electrode was fabricated through the PEDOT:PTS deposition technique outlined in Chapter Two, using gravure printing to deposit an oxidant and subsequent vapour phase polymerisation of the EDOT monomer.

The two electrodes of the cell were sealed using a 25 micron thick Dupont Surlyn film (USA), which served as both an adhesive and a spacer between the two electrodes. The cell was then back filled with electrolyte. The electrolyte was made up using a cobalt^(II/III)tris(bypyridyl)-based redox electrolyte previously reported in the literature[1]. The electrolyte was composed of 0.165 M cobalt^{II} tris(bypyridyl) (Dynamo, Sweden), 0.045 M cobalt^{III} tris(bypyridyl) (Dyename, Sweden), 0.8 M *tert*-butyl pyridine (Aldrich, USA) and 0.1 M LiClO₄ (Sigma Aldrich, USA) in an acetonitrile solvent. Impedance spectra of this cells was recorded over a seven day period using a Zahner Zennium electrochemical workstation ECW IM6 was used as a frequency response analyser. Data was analysed using Zview equivalent circuit modelling software (Scribner).

5.1.2 Results and Discussion

The resulting impedance spectra are shown in Figure 5.1.

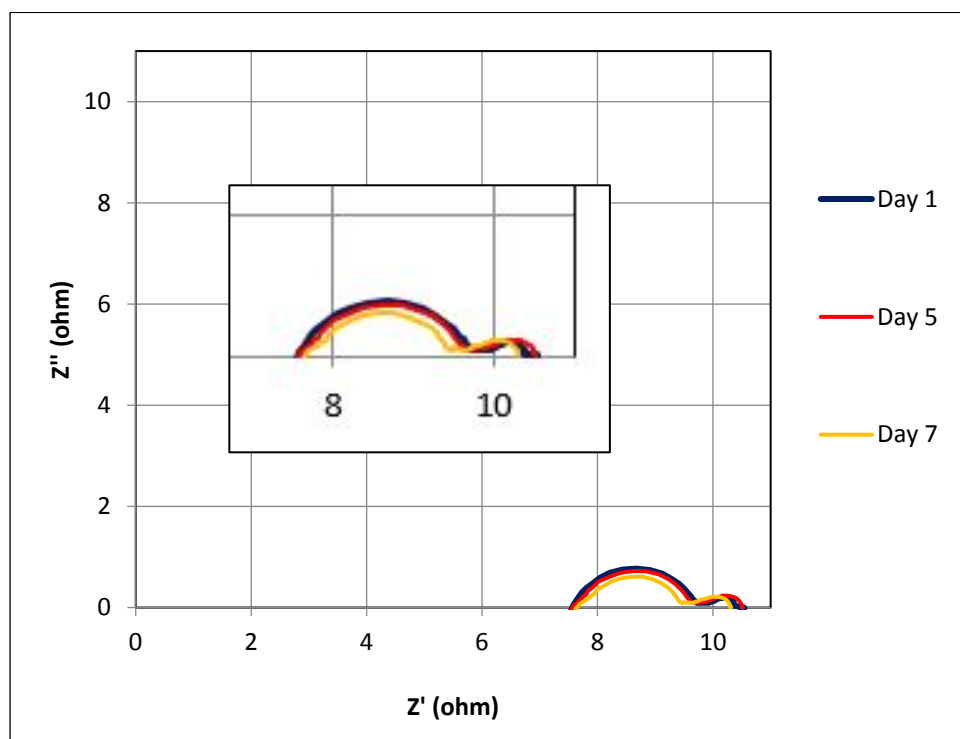


Figure 5.1. Nyquist plots of impedance spectra of a cell containing one glass/FTO/Pt electrode and one Ni/PEDOT-PTS electrode over seven days using a cobalt^(II/III)tris(bypyridyl)-based redox electrolyte.

In this investigation, it is not possible to conclusively assign each semicircle to a particular phenomenon occurring within the cell as done previously in Chapter 3. Although the literature can give some guidance[2], literature references discuss impedance spectroscopy results from DSSCs; the cell discussed here is not identical to a DSSC as this cell does not contain a working electrode. So, although literature references can give some clues as to elucidation of the spectra, this information can be used as a guide only. Furthermore, only one cell is tested here, unlike the similar study described in Chapter 3 in which there were three variations on an asymmetric cell. When three variations were tested, it was possible to observe which semicircle varied when a certain cell component was varied and assign that semicircle accordingly. This “process of elimination” elucidation method was not possible in

this case as only one asymmetric cell was tested. The full set of cells tested in Chapter Three were not tested here due to time and equipment constraints. Rather, this single set of EIS experiments was carried out to determine whether or not, in light of unstable results presented in the previous two chapters, use and optimisation of the Ni/PEDOT counter electrode should be pursued.

The Nyquist impedance plots of this cell appear to show two semicircles in the first spectrum recorded, on day one, and then three semicircles in the spectra recorded thereafter. However, it seems likely that this small, high frequency semicircle is also present in the first spectra, but is not apparent as it has been eclipsed by the centre semicircle. Evidence leading to this conclusion are, first, that the starting points of the spectra are virtually identical to each other. This indicates that, although not plainly visible on the spectra, the highest frequency semicircle is likely to be present in the first spectrum, similar to the subsequent spectra. Also, in the spectra recorded after five days and seven days the centre semicircle has progressively decreased in magnitude as time has elapsed, thus revealing the shoulder of a small semicircle at the highest frequency ($Z=7.9$ ohm).

According to Kern *et al.* [2, 3], the two semicircles at the higher frequencies, i.e. the first beginning at approximately $Z=7.5$ ohm, of which only a shoulder is visible on the spectra, can be attributed to interactions occurring at the electrodes. The semicircle at the lowest frequency can, from the literature, be attributed to diffusion within the electrolyte. Again, this information is in reference to complete DSSCs, so it is not directly applicable to this study.

Although the semicircles cannot be conclusively assigned to a component of the cell, information that can be gleaned from Figure 5.1 is that the system is stable in comparison to the experimental systems investigated in Chapter Three and Chapter Four. There are several points to note from the stability of this system. First, the starting point of all three spectra is consistent at around $Z=7.5$ ohm. This indicates that there is no change in the sheet resistance of the system over the seven day testing period, conclusively determining that corrosion is not occurring within the system. Second, the phenomenon of the PEDOT:PTS layer swelling in the electrolyte solvent seems to be less pronounced in this

system. This is surmised from the spectra as there is no instability within the system of comparable magnitude to that seen resulting from PEDOT:PTS swelling with MPN, as seen in Chapter 3. It appears that uptake of MPN by PEDOT:PTS is greater than uptake of acetonitrile, which is the solvent used here, by PEDOT:PTS.

5.1.3 Conclusion

The results from this preliminary investigation indicate that the nickel conducting substrate in the test electrode is compatible for use in a DSSC with an electrolyte containing a $\text{Co}^{2+}/\text{Co}^{3+}$ redox couple in conjunction with an acetonitrile electrolyte, with respect to corrosion behaviour of the system.

Chapter 5 References

1. Yella, A., *et al.*, *Porphyrin-Sensitized Solar Cells with Cobalt (II/III)-Based Redox Electrolyte Exceed 12 Percent Efficiency*, in *Science*. p. 629-634.
2. Kern, R., *et al.*, *Modeling and interpretation of electrical impedance spectra of dye solar cells operated under open-circuit conditions*. *Electrochimica Acta*, 2002. **47**(26): p. 4213-4225.
3. Wang, Q., J.E. Moser, and M. Gratzel, *Electrochemical impedance spectroscopic analysis of dye-sensitized solar cells*. *Journal of Physical Chemistry B*, 2005. **109**(31): p. 14945-14953.

Chapter 6: Conclusions and Further Work

6.1 Conclusions

Through this study it was concluded that a printed, flexible counter electrode for DSSCs can be fabricated using nickel foil and PEDOT:PTS. The catalytic PEDOT:PTS layer was successfully deposited onto both the conductive, flexible nickel sheet and a coating deposited from a commercial formulation of nickel flakes in acrylic binder coated onto PET film. Gravure printing of an oxidant formulation and subsequent vapour phase polymerisation of EDOT monomer were successfully used to deposit the PEDOT:PTS coating on both types of nickel surface. Only preliminary tests were carried out using the commercial nickel coating on PET as the conductive substrate, while further testing was carried out using the nickel sheet substrate. Preliminary tests on the PET/nickel coating indicated that there were inherent surface variability issues associated the formulation used to deposit the nickel film irrespective of care taken when preparing the coating. This variability served to introduce a high degree of irreproducibility into the results. For simplification, nickel foil was used as the substrate after this variability was discovered.

Upon observation of the behaviour of the nickel/PEDOT:PTS electrode in a cell with a DSSC electrolyte based on the iodide/triiodide redox couple, it was suspected that the nickel in the electrode was being corroded by the iodine species contained in the electrolyte. This corrosion was confirmed using the electrochemical methods of cyclic voltammetry and EIS. Marked changes in the impedance spectra resulting from decomposition of nickel due to corrosion were noted just five hours after cell fabrication. Tafel plots were constructed from cyclic voltammetry data and further validated the theory that the nickel was being corroded by the iodide/triiodide redox couple. In addition, wet chemistry methods further proved that corrosion of nickel occurred upon use of the experimental nickel/PEDOT:PTS together in a cell with an electrolyte containing the iodide/triiodide redox couple. In these wet chemistry tests, nickel was found to be dissolved in the electrolyte solution and iodine was found deposited on the surface of the nickel electrode. It had been previously reported in the literature that nickel showed good stability for three months in an iodide/triiodide electrolyte solution with an MPN solvent[1].

After this extensive testing was carried out on cells containing the nickel/PEDOT:PTS electrode together with the an electrolyte based on the iodide/triiodide redox couple, it was concluded that these two components are incompatible with each other. It is not possible to successfully use the Ni/PEDOT:PTS electrode in a DSSC in conjunction with an iodide/triiodide electrolyte. This finding is contrary to a stability report published in the literature of nickel in an iodide/triiodide based electrolyte with an MPN solvent[1], similar to that used in this thesis.

Through the course of this study, it was observed that the electrolyte used to fabricate the cells degraded over time. This was likely due to coordination of the thiocyanate anion with iodine, affecting the original chemical concentrations within the electrolyte. The electrolyte did not perform reliably for a period of longer than two weeks. As such, even if the every other component of a DSSC cell was stable, use of this electrolyte would introduce intrinsic instability into the system.

Further testing on this system consisted of determining whether or not the PEDOT:PTS catalytic coating swelled in the MPN electrolyte solution and, if so, quantifying this swelling. It was found that the PEDOT:PTS coating swelled with MPN to a maximum of a 112% of its original mass after nine days. The magnitude of swelling of the coating became stable after 30 days at 109% of its original mass. Although this phenomenon would serve to introduce instability into the cell immediately after fabrication, the initial equilibration period appears to last 30 days, after which the system is stable with respect to this aspect. In the event that a cell of this type was commercialised, this inherent phenomenon could be factored into its production. The equilibration period would likely occur during the storage and transportation of the product. By the time the cell was in service, stability with respect to PEDOT:PTS swelling would have been reached.

To determine whether or not the nickel/PEDOT:PTS counter electrode can be used in a DSSC, albeit not in conjunction with an iodide/triiodide based electrode, testing was conducted using the electrode with an electrolyte employing a less corrosive redox couple. The cobalt^{III} redox couple was used in the electrolyte with an acetonitrile solvent. It was found that the system was comparatively stable over a seven day testing period, indicating that the nickel/PEDOT:PTS electrode can potentially be used with an alternate redox electrolyte in a DSSC. The comparative stability of the system also indicates that the phenomenon of PEDOT:PTS swelling is less pronounced when the electrolyte solvent is acetonitrile than when the solvent is MPN. Further optimisation of the cell components could enhance stability of the system.

Nickel, in various forms, has been used in reported studies as a DSSC counter electrode component together in a cell with an iodide/triiodide electrolyte[2-4]. However, none of these studies reported corrosion of nickel. This is likely due to long term durability tests not being carried out and only one cell measurement being taken soon after cell fabrication, i.e. before a significant amount of corrosion had occurred.

Further work on this alternate counter electrode would be centred primarily around optimisation of the nickel/PEDOT:PTS electrode and fine tuning of the electrolyte, with respect to the redox couple and the solvent, to yield the optimum results in terms of light to energy conversion and long term stability.

6.2 Future Work

A comprehensive EIS study, similar to the study described in Chapter 3, should be conducted on the system containing the nickel/PEDOT:PTS electrode together with an electrolyte based on the Co(II/III) redox couple and an acetonitrile solvent. This would allow deconvolution and further characterisation of the system. In addition, a swelling experiment similar to that described in Chapter 4, should be conducted to conclusively quantify both the magnitude of swelling with acetonitrile the PEDOT:PTS coating experiences and the time it takes to reach stability regarding swelling. An additional aspect that would be useful to consider is whether or not swelling of the PEDOT:PTS coating with electrolyte solvent affects the adherence of the coating to the conductive nickel foil and what, if any, implications this has on cell performance and longevity. Furthermore, whether or not swelling of the PEDOT:PTS polymer has an effect on its catalytic behaviour should be determined.

To optimise the alternate counter electrode performance, an investigation of the effect that morphology of PEDOT:PTS has on cell performance could be conducted. There have been multiple reports indicating that the porosity of the catalytic layer on the DSSC counter electrode is a crucial factor in determining performance[5-7]. Tailoring pore size and shape of the catalytic layer to suit the reduction reaction required is also likely to impact counter electrode performance. The specific reduction reaction occurring at the counter electrode will, of course, depend on the redox couple used in the electrolyte.

In Chapter Two of this thesis, printing of multiple layers of PEDOT:PTS was carried out with the aim of increasing PEDOT:PTS layer thickness. In turn, it was hoped that a greater surface area of PEDOT:PTS would be available for catalytic activity. This multiple layer printing was abandoned as it was deemed irreproducible. In light of the many reports indicating that increasing the surface area of this catalytic layer would enhance the counter electrode, it would be useful to find a way that this concept of printing or coating multiple layers can be successfully carried out. One method to attempt is to carry out the entire VPP process between each layer being printed, rather than apply three layers of oxidant to the substrate and carry out one polymerisation process as was done here.

Morphology of the PEDOT:PTS coating will be different depending on the deposition method used. Some different deposition methods that could be investigated include bar coating, slot die coating and spin coating (although spin coating is a non-scalable deposition technique, so there is little scope to use it industrially). If this investigation was to be carried out, the PEDOT:PTS film deposited using each method should be characterised using scanning electron microscopy imaging, X-ray photoelectron spectroscopy (XPS) and UV-visible spectrophotometry.

The printed, flexible nickel/PEDOT:PTS DSSC counter electrode investigated here has the potential to contribute to the establishment of faster, lower cost fabrication of DSSCs. The use of this novel electrode could circumvent the requirement for high monetary cost material and high energy cost processes. Furthermore fabrication of flexible, lighter weight cells would open DSSCs up to be used as a portable energy source, making them suited to integration into consumer products such as bags or small electrical devices.

Chapter 6 References

1. Ma, T.L., *et al.*, *Properties of several types of novel counter electrodes for dye-sensitized solar cells*. Journal of Electroanalytical Chemistry, 2004. **574**(1): p. 77-83.
2. Jiang, Q.W., *et al.*, *Surface-Nitrided Nickel with Bifunctional Structure As Low-Cost Counter Electrode for Dye-Sensitized Solar Cells*. Journal of Physical Chemistry C. **114**(31): p. 13397-13401.
3. Sun, H.C., *et al.*, *Dye-sensitized solar cells with NiS counter electrodes electrodeposited by a potential reversal technique*. Energy & Environmental Science, 2011. **4**(8): p. 2630-2637.
4. Wang, H., W. Wei, and Y.H. Hu, *NiO as an Efficient Counter Electrode Catalyst for Dye-Sensitized Solar Cells*. Topics in Catalysis, 2014. **57**(6-9): p. 607-611.
5. Sirimanne, P.M., *et al.*, *Towards an all-polymer cathode for dye sensitized photovoltaic cells*. Thin Solid Films. **518**(10): p. 2871-2875.
6. Saito, Y., *et al.*, *Application of poly(3,4-ethylenedioxythiophene) to counter electrode in dye-sensitized solar cells*. Chemistry Letters, 2002(10): p. 1060-1061.
7. Chen, J.G., H.Y. Wei, and K.C. Ho, *Using modified poly(3,4-ethylene dioxythiophene): Poly(styrene sulfonate) film as a counter electrode in dye-sensitized solar cells*. Solar Energy Materials and Solar Cells, 2007. **91**(15-16): p. 1472-1477.